STUDY OF THERMODYNAMIC BINDING BETWEEN ADER AND ADES IN TWO-COMPONENT ANTIBIOTIC SENSOR OF ANTIBIOTIC RESISTANT STRAINS OF *ACINETOBACTER BAUMANNII*

Miss Konrawee Thananon

A Thesis Submitted in Partial Fulfillment of the Requirements
for the Degree of Master of Science in Medical Microbiology (Interdisciplinary Program)
Medical Microbiology,Interdisciplinary Program
GRADUATE SCHOOL
Chulalongkorn University
Academic Year 2022

การศึกษาเกี่ยวกับคุณสมบัติทางเทอร์โมไดนามิกส์ในการจับกันระหว่าง AdeR และ AdeS ในระบบของโปรตีนที่มีสององค์ประกอบที่เกี่ยวข้องกับการรับสัญญาณกระตุ้นโดยยาปฏิชีวนะของ *Acinetobacter baumannii* ในสายพันธุ์ที่ดื้อต่อยาปฏิชีวนะ

น.ส.กรรวี ธนานนท์

วิทยานิพนธ์นี้เป็นส่วนหนึ่งของการศึกษาตามหลักสูตรปริญญาวิทยาศาสตรมหาบัณฑิต
สาขาวิชาจุลชีววิทยาทางการแพทย์ (สหสาขาวิชา) สหสาขาวิชาจุลชีววิทยาทางการแพทย์
บัณฑิตวิทยาลัย จุฬาลงกรณ์มหาวิทยาลัย
ปีการศึกษา 2565

Thesis Title	STUDY OF THERMODYNAMIC BINDING BETWEEN ADER AND ADES IN TWO-COMPONENT ANTIBIOTIC SENSOR OF ANTIBIOTIC RESISTANT STRAINS OF *ACINETOBACTER BAUMANNII*
By	Miss Konrawee Thananon
Field of Study	Medical Microbiology (Interdisciplinary Program)
Thesis Advisor	Associate Professor PATCHAREE RITPRAJAK, D.D.S., Ph.D.
Thesis Co Advisor	Associate Professor JEERUS SUCHARITAKUL, D.D.S., Ph.D.

Accepted by the GRADUATE SCHOOL, Chulalongkorn University in Partial Fulfillment of the Requirement for the Master of Science

..... Dean of the GRADUATE SCHOOL
(Associate Professor YOOTTHANA CHUPPUNNARAT, Ph.D.)

THESIS COMMITTEE

..... Chairman
(Associate Professor KANITHA PATARAKUL, M.D., Ph.D.)

..... Thesis Advisor
(Associate Professor PATCHAREE RITPRAJAK, D.D.S., Ph.D.)

..... Thesis Co-Advisor
(Associate Professor JEERUS SUCHARITAKUL, D.D.S., Ph.D.)

..... Examiner
(WONGSAKORN PHONGSOPITANUN, Ph.D.)

..... External Examiner
(Panu Pimviriyakul, Ph.D.)

กรรวี ธนานนท์ : การศึกษาเกี่ยวกับคุณสมบัติทางเทอร์โมไดนามิกส์ในการจับกันระหว่าง AdeR และ AdeS ในระบบของโปรตีนที่มีสององค์ประกอบที่เกี่ยวข้องกับการรับสัญญาณกระตุ้นโดยยาปฏิชีวนะของ *Acinetobacter baumannii* ในสายพันธุ์ที่ดื้อต่อยาปฏิชีวนะ. (STUDY OF THERMODYNAMIC BINDING BETWEEN ADER AND ADES IN TWO-COMPONENT ANTIBIOTIC SENSOR OF ANTIBIOTIC RESISTANT STRAINS OF *ACINETOBACTER BAUMANNII*) อ.ที่ปรึกษาหลัก : รศ. ทญ ดร.พัชรี ฤทธิ์ประจักษ์, อ.ที่ปรึกษาร่วม : รศ. ทพ. ดร.จีรัสย์ สุจริตกุล

โปรตีน AdeR (Response regulator) และ AdeS (histidine kinase) มีบทบาทสำคัญในการควบคุม efflux pump ซึ่งมีหน้าที่กำจัดยาปฏิชีวนะออกจากเซลล์แบคทีเรีย โดยจะเกิดขึ้นผ่านระบบควบคุมแบบสององค์ประกอบ (Two-component regulatory system; TCS) ที่เกี่ยวข้องกับออโตฟอสโฟรีเลชั่น ที่เมื่อได้รับสัญญาณจากภายนอก AdeS จะส่งสัญญาณผ่านการเกิดออโตฟอสโฟรีเลชั่นซึ่งนำไปสู่การกระตุ้น AdeR และจะเริ่มต้นการแสดงออกของยีนเป้าหมายที่เกี่ยวข้องกับ efflux pump โดยในการศึกษานี้ โปรตีน AdeR และ AdeS จากสายพันธุ์อ้างอิงของ *Acinetobacter baumannii* (ATCC19606) และสายพันธุ์ที่ดื้อยาปฏิชีวนะ (H1074 และ G560) ถูกโคลนและแสดงออกใน *E. coli* และเอนไซม์มีการติด His-tag ที่ C-terminus และถูกทำให้บริสุทธิ์โดยใช้คอลัมน์โครมาโตกราฟีที่มีไอออนของโลหะตรึงไว้ การศึกษานี้จะศึกษาคุณสมบัติที่แตกต่างในการจับกันระหว่าง AdeR และ AdeS ของสายพันธุ์ที่ดื้อต่อยาปฏิชีวนะและสายพันธุ์อ้างอิง โดยอาศัยวิธีการทดสอบการเคลื่อนที่ด้วยไฟฟ้า (EMSA) การถ่ายโอนพลังงานเรโซแนนซ์ฟลูออเรสเซนซ์ (FRET) การวัดปริมาณความร้อนด้วยการไตเตรทแบบไอโซเทอร์มอล (ITC) และกิจกรรมของเอนไซม์ที่เกิดขึ้น โดยผลลัพธ์ของ EMSA แสดงให้เห็นว่าทั้งสายพันธุ์อ้างอิงและสายพันธุ์ที่ดื้อต่อยาปฏิชีวนะมีความสามารถในการจับกับ intercistronic DNA การวิเคราะห์ FRET บ่งชี้ว่าการผสมของ AdeR ที่ติดฉลากด้วย Cy3 และ AdeS ที่ติดฉลากด้วย Cy5 แสดงความเข้มที่สูงกว่าที่ 485 นาโนเมตร เมื่อเทียบกับการผสมของ Cy3 และ Cy5 เพียงอย่างเดียว อย่างไรก็ตาม ไม่พบสัญญาณ FRET ระหว่าง donor และ acceptor ผลจาก ITC ไม่พบการจับกันระหว่าง AdeR และ DNA หรือระหว่าง AdeR และ AdeS ผลจากการทดสอบ kinase และ ATP hydrolysis ของ AdeS พบว่ามี ทั้ง kinase activity และ ATP hydrolysis และ โดยจากการศึกษานี้แสดงให้เห็นถึงความสามารถของ AdeR ในการจับ intercistronic DNA และปฏิสัมพันธ์ที่อาจเกิดขึ้นระหว่าง AdeR กับ AdeS อย่างไรก็ตาม ค่า binding affinity ที่แน่นอนไม่สามารถระบุได้ผ่าน ITC นอกจากนี้ การทดลอง FRET ไม่ได้ให้ผลที่สรุปถึงปฏิกิริยาระหว่างโปรตีนและโปรตีนซึ่งจำเป็นต้องมีการตรวจสอบเพิ่มเติมเพื่อทำความเข้าใจผลกระทบของการแปรผันของกรดอะมิโนของ AdeR เมื่อจับกับ DNA และความสัมพันธ์ของ AdeR และ AdeS ในการควบคุมการแสดงออกของ efflux pump โดยผลลัพธ์เหล่านี้มีความเกี่ยวข้องกับปฏิสัมพันธ์ของโปรตีนในระบบการกำกับดูแลสององค์ประกอบนี้เพื่อลดการดื้อยาใน *A. baumannii*

สาขาวิชา	จุลชีววิทยาทางการแพทย์ (สหสาขาวิชา)	ลายมือชื่อนิสิต .....
ปีการศึกษา	2565	ลายมือชื่อ อ.ที่ปรึกษาหลัก .....
		ลายมือชื่อ อ.ที่ปรึกษาร่วม .....

6382002020 : MAJOR MEDICAL MICROBIOLOGY (INTERDISCIPLINARY PROGRAM)

KEYWORD: Acinetobacter baumannii, Two-component regulatory system, Response regulator, AdeR, Histidine kinase, AdeS

Konrawee Thananon : STUDY OF THERMODYNAMIC BINDING BETWEEN ADER AND ADES IN TWO-COMPONENT ANTIBIOTIC SENSOR OF ANTIBIOTIC RESISTANT STRAINS OF *ACINETOBACTER BAUMANNII*. Advisor: Assoc. Prof. PATCHAREE RITPRAJAK, D.D.S., Ph.D. Co-advisor: Assoc. Prof. JEERUS SUCHARITAKUL, D.D.S., Ph.D.

The proteins AdeR (response regulator) and AdeS (histidine kinase sensor) play a crucial role in regulating the efflux pump, which is responsible for removing antibiotics from bacterial cells. This regulation occurs through a two-component regulatory system (TCS) involving autophosphorylation. Upon receiving external signals, AdeS undergoes autophosphorylation, leading to the activation of AdeR, which in turn initiates the expression of target genes related to the efflux pump. In this study, both enzymes from the reference strain of *Acinetobacter baumannii* (ATCC19606) and antibiotic resistant strains (H1074 and G560) were cloned and expressed in *E. coli*. The enzymes were purified using an immobilized metal ion affinity chromatography (IMAC) column, utilizing a C-terminal His-tag. To investigate the interaction characteristics between the antibiotic resistant strains and the reference strain, several procedures were employed, including electrophoretic mobility shift assay (EMSA), fluorescence resonance energy transfer (FRET), isothermal titration calorimetry (ITC), and enzymatic activity assay. The EMSA results demonstrated that both the reference and antibiotic resistant strains were capable of binding to the intercistronic DNA. The FRET analysis indicated that the mixing of AdeR labeled with Cy3 and AdeS labeled with Cy5 exhibited a higher intensity at 485 nm compared to the mixing of Cy3 and Cy5 alone. However, no FRET signal indicating binding between the donor and acceptor was detected. Moreover, the ITC results did not detect any binding between AdeR and DNA or between AdeR and AdeS. The enzymatic activity assay found that AdeS has kinase activity and ATP hydrolysis. In this study, demonstrate the ability of AdeR to interact with the intercistronic DNA. And suggest the occurrence of potential interactions between AdeR and AdeS. However, the exact binding affinity could not be determined through ITC. Additionally, the FRET experiments did not provide conclusive evidence of protein-protein interactions. Further investigations are warranted to understand the effects of variations in amino acids on the affinity of AdeR for DNA and the affinity of AdeR and AdeS in controlling efflux pump expression. These results have implications for manipulating protein interactions in this system to minimize drug resistance in *A. baumannii*.

Field of Study:	Medical Microbiology (Interdisciplinary Program)	Student's Signature .....
Academic Year:	2022	Advisor's Signature .....
		Co-advisor's Signature .....

ACKNOWLEDGEMENTS

The author expresses sincere gratitude to their advisor, Assoc. Prof. Patcharee Ritprajak, D.D.S., Ph.D., from the Department of Microbiology, Faculty of Dentistry, Chulalongkorn University, as well as co-advisor Assoc. Prof. Jeerus Sucharitakul, D.D.S., Ph.D., from the Department of Biochemistry, Faculty of Dentistry, Chulalongkorn University. The author would also like to thank Dr. Worrapoj Oonanant from the Department of Basic Medical Science, Faculty of Medicine Vajira Hospital, Navamindradhiraj University, and Dr. Panu Pimviriyakul from the Department of Biochemistry, Faculty of Science, Kasetsart University, for their guidance, support, and contributions to the research. Special thanks are extended to Kanyarat, Aunchiya and Phawida for their assistance in various matters, including laboratory work. The author is grateful to the Oral Biology Research Center, Faculty of Dentistry, Chulalongkorn University, for providing essential research equipment and facilities. The author would also like to express gratitude to their family for their unwavering support, as well as to the members of Bangtan for being a source of inspiration and brightness during challenging times. Thank you so much.

Konrawee Thananon

TABLE OF CONTENTS

Page

..... iii

ABSTRACT (THAI) iii

..... iv

ABSTRACT (ENGLISH) iv

ACKNOWLEDGEMENTS v

TABLE OF CONTENTS vi

LIST OF TABLES ix

LIST OF FIGURES x

CHAPTER I INTRODUCTION 1

CHAPTER II HYPOTHESIS AND OBJECTIVES 3

Research question 3

Research objectives 3

CHAPTER III LITERATURE REVIEWS 4

Acinetobacter baumannii 4

Mechanisms of antibiotic resistance in *A. baumannii* 6

Modification of antibiotic chemical structures that have been directly modified 6

The occurrence of cell membrane defects resulting in antibiotic permeability. 6

Mutation of the antibiotic-targeted proteins. 7

Activation of efflux pumps for drug excretion. 7

The multidrug and toxic compound extrusion (MATE) family. 7

The adenosine triphosphate (ATP)-binding cassette (ABC) superfamily. 7
The small multidrug resistance (SMR) family. 7
The major facilitator (MFS) superfamily. 7
The resistance-nodulation-cell division (RND) family. 8
AdeABC efflux pump 9
Two-component regulatory systems (TCSs) 10
Investigation of the protein structures 11
Structure of Response regulator (AdeR) 11
Structure of Histidine kinase (AdeS) 12
CHAPTER IV METHODOLOGY 13
Conceptual framework 13
CHAPTER V MATERIALS AND METHODS 14
Bacterials strains selection 14
Construction of expression vectors for AdeR and AdeS 14
DNA primers for *adeR* gene 15
Protein expression 16
Purification of AdeR 16
Purification of AdeS 17
Measured the size of the protein using Fast protein liquid Chromatography 18
Preparation of DNA for AdeR binding 18
Electrophoretic mobility shift assay (EMSA) 19
Isothermal titration calorimetry (ITC) 19
Enzymatic activity assay 21
ATP hydrolysis from kinase activity of histidine kinase 21

Malachite green Phosphate Assay 22
Protein-dye labeling 23
Forster or fluorescence resonance energy transfer (FRET) 23
CHAPTER VI RESULTS 24
Protein purification and expression 24
1.1 Purification and expression of full-length AdeR (ATCC19606) and antibiotic resistant strains AdeR (H1074 and G560) 24
1.2 Purification and expression of truncated AdeS (ATCC19606) and antibiotic resistant strains AdeS (H1074 and G560) 28
Investigation of the interaction of AdeR and DNA using EMSA and ITC 31
Electrophoretic mobility shift assay (EMSA) of AdeR-DNA complex 31
Isothermal titration calorimetry (ITC) of AdeR-DNA complex 34
Investigation of the interaction between AdeR and AdeS using FRET 37
Kinase activity assay of AdeS 44
Investigation of Protein-Protein Interactions using Isothermal Titration Calorimetry 47
CHAPTER VII DISCUSSION 49
APPENDIX A MATERIALS AND EQUIPMENT 54
APPENDIX B BIOLOGICAL/CHEMICAL AGENTS AND REAGENTS 56
APPENDIX C SOFTWARE AND DATABASE 59
APPENDIX D REAGENT PREPARATION 60
REFERENCES 62
VITA 69

LIST OF TABLES

Page

Table 1. Examples of virulence factors of A. baumannii (9, 25, 28, 29)..... 5

Table 2. Primers for truncated AdeS. 15

Table 3. Primers for AdeR. 15

Table 4. ATP hydrolysis from kinase activity assay..... 21

Table 5. Phosphate standard curve..... 22

Table 6. Results of enzymatic activity assay (coupling assay) 44

LIST OF FIGURES

Page

Figure 1. A. baumannii 4

Figure 2. Five main Multidrug efflux pumps (MDEPs) with their well-known examples and antibiotic substrates. 8

Figure 3. Operons for RND family efflux pump systems in A. baumannii. 9

Figure 4. Two-component regulatory system 11

Figure 5. Two-component regulatory system 12

Figure 6. Coupling reaction for kinase activity assay. 21

Figure 7. Protein expression and purification using IMAC sepharose. 25

Figure 8. The chromatogram of standard protein molecular weights. 26

Figure 9. Determination native form of AdeR 27

Figure 10. Protein expression and purification using IMAC sepharose. 29

Figure 11. Determination native form of AdeS 30

Figure 12. The EMSA results of the binding of DNA with AdeR ATCC19606 reference strain and antibiotic resistant strain H1074 and G560 on the intercistronic region. 32

Figure 13. Isothermal titration calorimetry of AdeR ATCC19606 to 3.96 nM of DNA .. 35

Figure 14. Isothermal titration calorimetry of AdeR ATCC19606 to 892.65 nM of DNA 36

Figure 15. Excitation and emission spectra of AdeR (ATCC19606) labeled with Cy3 and AdeS (ATCC19606) labeled with Cy5. 38

Figure 16. Emission spectra of FRET from interaction between AdeR-Cy3 (ATCC19606) and AdeS-Cy5 (ATCC19606). 38

Figure 17. 1 μM Cy3 titrated with Cy5 40

Figure 18. 1 μM AdeR-Cy3 (ATCC19606) titrated with AdeS-Cy5 (ATCC19606) 40

Figure 19. 1 μM Cy3 titrated with AdeS-Cy5 (ATCC19606) 42

Figure 20. 1 μM AdeR-Cy3 (ATCC19606) titrated with Cy5 42

Figure 21. Plot a graph illustrating the correlation between concentration and intensity. 43

Figure 22. Spectrum of the Phosphate standard 45

Figure 23. Standard Curve of Phosphate Standard 45

Figure 24. Spectrum of the Malachite Green used for Phosphate assay of AdeS. 46

Figure 25. Spectrum of the Resulting Phosphate by Comparing Phosphate Standards (10 – 80 μM) and AdeS. 46

Figure 26. Isothermal titration calorimetry of buffer to buffer 48

CHAPTER I

INTRODUCTION

Antibiotic resistance in *Acinetobacter baumannii* is a serious concern. It has been discovered that antimicrobial-resistant strains increase mortality and pose a serious problem for intensive care unit (ICU) patients, posing a significant challenge for physicians and medical staff in terms of eliminating infection in the hospital or in the community (1-9). There are several antibiotics such as carbapenems, cephalosporins, and imipenem which are used were among the first antibiotics used to treat the infection caused by *A. baumannii* (4, 7, 10).

There are several mechanisms of *A. baumannii* for increasing ability of antimicrobial resistance, such as biofilm formation, outer membrane porin (6) factors, and the secretion of disease-causing enzymes such as phospholipase. It also has antibiotic resistance mechanisms involved in multidrug efflux pumps (2, 9). Extensively drug resistant *A. baumannii* (XDR-Ab) refers to strains that resistant to two drug classes, Multidrug resistant *A. baumannii* (MDR-Ab) refers to strains that are resistant to three or more antimicrobial drug classes, and Pan drug resistant *A. baumannii* (PDR-Ab) refers to strains that resistant to all drug classes (11).

Efflux pumps play an important role in the excretion of drugs out of bacterial cells. AdeABC efflux pump is one of efflux systems in the resistance-nodulation-cell division (RND family), which transport antibiotics or cytotoxic substances out of bacterial cells via proton-motive-force-dependent transport (9, 12-19). The most research study is AdeABC efflux pump (20). The AdeABC efflux pump is composed of three components: membrane fusion protein (AdeA), transmembrane (AdeB) and outer membrane channel protein (AdeC). The genes for those protein expression are controlled by a two-component regulatory system (TCS) which are a response regulator (RR or AdeR) and histidine kinase sensor (HK or AdeS) (15, 20-22).

TCS is composed of two proteins, the response regulator (AdeR) and the histidine kinase sensor (AdeS), which regulate via autophosphorylation. When AdeS

receives a signal from the outside, the signal is transferred to AdeR, which causes a response up (23, 24).

A. baumannii is one of the most pathogens found in hospital infections due to the high prevalence of infection and the shortage of effective antibiotics for treatment. To overcome this problem knowledge of antibiotic resistance mechanisms and pathogenic factors is needed.

There are evidences for increasing in gene expression of Ade pump which is controlled by AdeR and AdeS (4, 9, 12, 21). In antibiotic resistant strains of *A. baumannii* show more potentials for antibiotic resistance than the reference strain (4). This finding leads to an investigation of the different protein interaction between the two-component regulatory system. This study is to investigate different properties of the interaction of the antibiotic resistant strains and the reference strain (ATCC19606), the antibiotic resistant strains of H1074 and G560. Both strains were isolated from patients (H1074 from hemoculture, G560 from urine) with the antibiotic resistance *A. baumannii* infection in the Faculty of Medicine Vajira Hospital Navamindradhiraj University. The knowledge from the study leads to manipulate the interaction between two components of AdeR and AdeS to inhibit or minimize expression of efflux pump systems which are controlled by the two-component regulatory system.

CHAPTER II

HYPOTHESIS AND OBJECTIVES

Research question

1. How AdeR of antibiotic resistant strains effect on binding to DNA.
2. How antibiotic resistant strains effect on protein-protein interaction between AdeR and AdeS.

Research objectives

1. To study binding affinity of AdeR to DNA, and compare between antibiotic resistant strains and reference strain.
2. To study interaction between AdeR and AdeS, and compare between antibiotic resistant strains and reference strain.
3. To investigate an effect of AdeR on AdeS kinase activity and compare between antibiotic resistant strains and reference strain.

CHAPTER III

LITERATURE REVIEWS

Acinetobacter baumannii

Acinetobacter spp. is a Gram-negative coccobacillus, aerobic, non-motile, and glucose-non-fermentative that shown in figure 1 (2, 9).

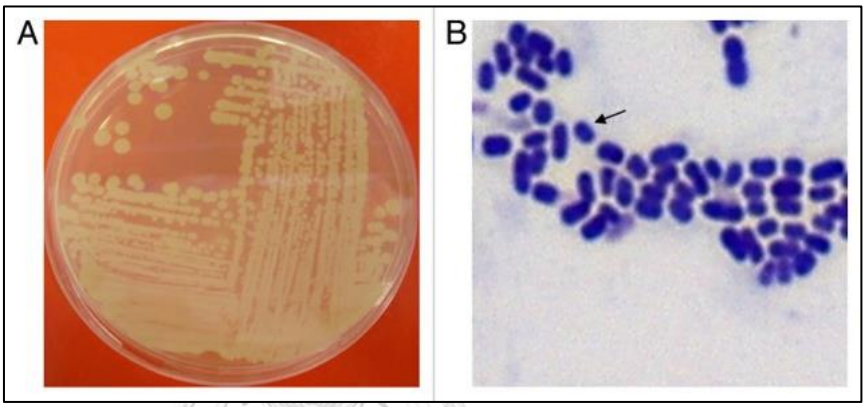

Figure 1. *A. baumannii*

(A) *A. baumannii* complex streak after overnight growth on Luria-Bertani agar at 37°C. and (B) Gram-stain of *A. baumannii* cells grown in Luria-Bertani broth. The arrow represents a single *A. baumannii* cell (2).

Acinetobacter baumannii is well-known as pathogenic bacteria. The microorganism can causes infections of skin, bloodstream, urinary tract, respiratory tract, and other soft tissues, particularly in ICU patients. Infection with *A. baumannii* is extremely dangerous because most of infected patients may need to stay in the hospital for an extended period (> 90 days), depending on the severity of symptoms (2, 3, 9). The microorganism has the unique ability to survive in hospitals and widespread epidemic. The World Health Organization (WHO) and the Infectious Diseases Society of America (IDSA) designated *A. baumannii* as the sixth danger that must be closely monitored (2, 4-6). *A. baumannii* has several mechanisms that cause diseases or various virulence factors, such as OmpA which is protein can induce

apoptosis of host cells, biofilm formation, secretion of *A. baumannii* enzymes such as phospholipases (phospholipase C, D), proteases, or protein secretion systems, including the iron-chelating systems in Table 1 (2, 9, 25). These diverse mechanisms result in A. *baumannii* combating to a wide range of antibiotics, including cefoxitin, ceftazidime, imipenem, aztreonam, ciprofloxacin, gentamicin, tigecycline, and colistin (4, 6, 25-27).

Table 1. Examples of virulence factors of *A. baumannii* (9, 25, 28, 29).

Virulence factor	**Purpose role in pathogenesis**
Porins; OmpA	Adherence and invasion, inducing apoptosis, biofilm formation, extrusion of antibiotics from the periplasmic space through the outer membrane collaborating with inner membrane efflux systems
Lipopolysaccharide (LPS)	Persistent tissue infection, evasion of the host immune response
Phospholipase	Invasion, in *vivo* survival, toxicity to epithelial cells
Capsular Polysaccharide Composition and Outer Membrane Resistance to Desiccation and Disinfection	Providing defense against the environment
Biofilm formation	Causing the microorganism to be multidrug resistant

Mechanisms of antibiotic resistance in *A. baumannii*

As *A. baumannii* was resistant to that antimicrobial drug. Until being classified as XDR, MDR and PDR-*A. baumannii* is caused by its own antibiotic resistance mechanism. In this section, we will look at the mechanisms that cause *A. baumannii* to become resistant to various antibiotics. As an example, consider the following (30):

Modification of antibiotic chemical structures that have been directly modified

A. baumannii can destroy or modify the antibiotics *via* hydrolysis, which is an enzyme-catalyzed conversion of the antibiotic. Enzymatic hydrolysis of β-lactam ring is the main mechanism. The β-lactamases breaks down antibiotic containing β-lactams such as penicillin, cephalosporins, clavams, carbapenems, and monobactams. *A. baumannii* antibiotic modification is detrimental to the treatment of hospital-acquired infections, eventually leading to the development of antibiotic resistance (9, 31).

The occurrence of cell membrane defects resulting in antibiotic permeability.

Cell membrane of Gram-negative bacteria *A. baumannii* is less permeable than gram-positive bacteria. Porins are outer membrane proteins associated with modulating cellular permeability. The outer membrane acts as a barrier to penetration. Many antibiotics become less permeable because of the presence of porins such as OmpA, a protein responsible for transporting molecules across lipid bilayer membranes. The protein also plays a major role in adherence and invasion of epithelial cells by interacting with fibronectin and binds to factor H in human serum, which may allow *A. baumannii* to avoid complement-mediated killing. Furthermore OmpA is also involved in antimicrobial resistance because disrupting the *ompA* gene significantly decreases the minimal inhibitory concentrations (MICs) of several antibiotics (chloramphenicol, aztreonam, and nalidixic acid), suggesting that OmpA participates in the extrusion of antibiotics from the periplasmic space through the outer membrane and couples with inner membrane efflux systems (9, 16, 23).

Mutation of the antibiotic-targeted proteins.

Most antibiotics specifically bind to their targets with high affinity. The mutation of antibiotic-targeted proteins potentially has less affinity or no binding. For example, the overexpression of penicillin binding protein (PBP) results in low affinity to the drug, leading to better antibiotic resistance (9, 31).

Activation of efflux pumps for drug excretion.

Efflux pumps are associated with resistance against many different classes of antibiotics, such as imipenem and tigecycline. When those genes are overexpressed, the drug is excreted from within the cell to the outside, causing the bacteria to become antibiotic resistant (9, 12, 16, 29, 31, 32). It was discovered that efflux pumps can be classified into five major groups, that shown in figure 2 as follows:

The multidrug and toxic compound extrusion (MATE) family.

MATE family is an efflux pump that transports drugs or cytotoxic substances out of the cell *via* proton-motive-force and sodium ion gradient, such as AbeM, This system uses proton stimulation to drive the antibiotic out of the cell (12-14).

The adenosine triphosphate (ATP)-binding cassette (ABC) superfamily.

ABC superfamily is an efflux pump that transports drugs out of cells *via* ATP hydrolysis. This family is mostly found in gram-positive bacteria, such as the Sav1866 multidrug exporter in *S. aureus* (12-14, 22).

The small multidrug resistance (SMR) family.

SMR family such as EmrE from *E. coli* is an efflux pump that transports drugs out of the cell via a proton-motive-force-dependent mechanism (12, 14).

The major facilitator (MFS) superfamily.

MFS family such as Tet efflux pumps is an efflux pump with a proton-motive-force-dependent function that transports drugs out of the cell. The MFS efflux pumps are not normally multidrug transporters but the system functions as specific exporters of certain classes of antimicrobial agents because it is specific to some antibiotics, such as tetracycline (12-14).

The resistance-nodulation-cell division (RND) family.

RND family is an efflux pump that transports drugs out of the cell via a proton-motive-force-dependent mechanism. This family is only existed in Gram-negative bacteria. Efflux pumps are found within the inner membrane of Gram-negative bacteria and collaborate with two other proteins: the outer membrane channel and the periplasmic adapter protein to form a tripartite efflux pump that covers both the inner and outer membranes (9, 12-19).

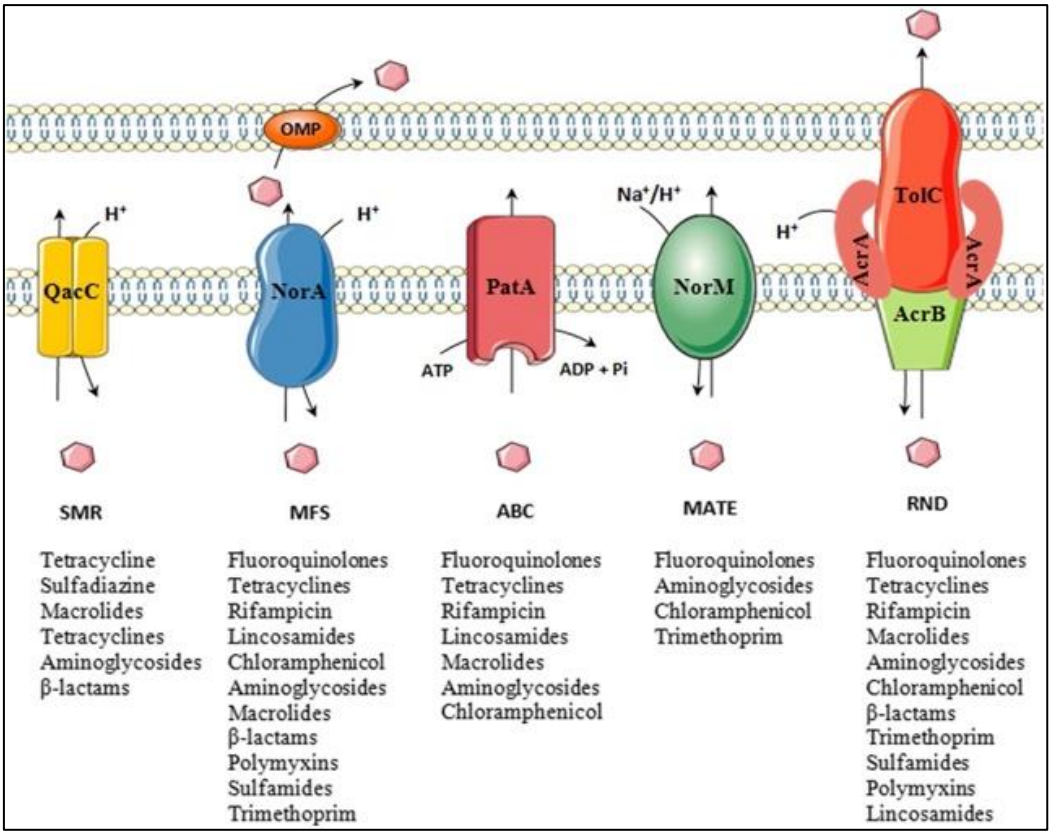

Figure 2. Five main Multidrug efflux pumps (MDEPs) with their well-known examples and antibiotic substrates.

OMP: outer membrane protein; SMR: the small multidrug resistance family; MFS: the major facilitator superfamily; ABC: ATP-binding cassette superfamily; MATE: the multidrug and toxic compound extrusion family and RND: the resistance-nodulation-division family (13).

In *A. baumannii*, antibiotic resistance caused by efflux pumps is frequently associated with the MFS and RND families, and the efflux pumps found in the RND family are AdeABC, AdeFGH, and AdeIJK (4, 12, 13, 18-21).

AdeABC efflux pump

AdeABC efflux pump is a member of the RND family, which is involved in the antibiotic resistance mechanism of bacteria. AdeABC efflux pump is composed of three major components: an inner membrane transporter or transmembrane component (AdeB), a membrane fusion protein (AdeA), and an outer membrane channel protein (AdeC). AdeABC is encoded from the *adeABC* genes, which controlled by a two-component system. The system composed of a sensor kinase (AdeS) and a response regulator (AdeR) separated by an intercistronic spacer (ICS) as shown in figure 3 (1, 20-22, 27, 33).

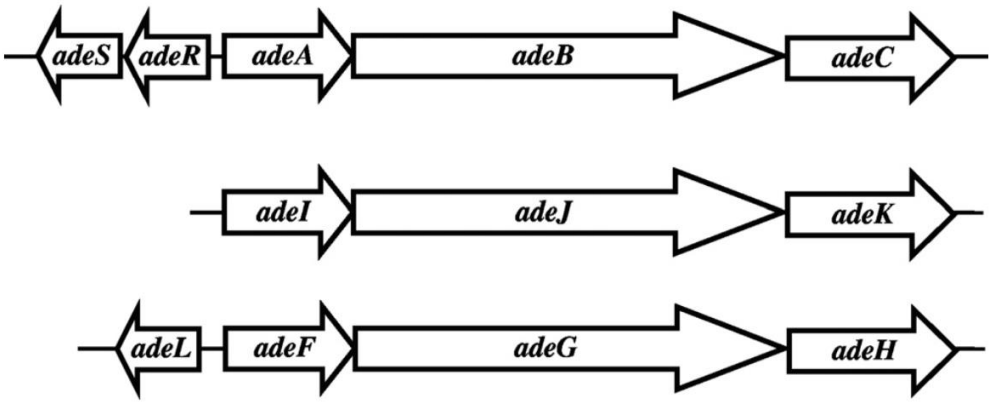

Figure 3. Operons for RND family efflux pump systems in *A. baumannii.*
Coding sequences are represented by open arrows, which also show the direction of transcription (20).

Two-component regulatory systems (TCSs)

TCSs are triggered by a variety of stimulants in environment outside such as antibiotics and intra-host conditions. Genes such as AdeRS that found in TCSs play an important role for important functions or are involved in a control of key expressions such as pathogenic roles, biofilm formation, and multidrug efflux activity (23, 24). TCSs are composed of a kinase sensor and a response regulator. As shown in Figure 4, TCSs contains histidine kinase (AdeS), also response regulator (AdeR) (1, 24). The AdeS detects environmental changes and transfers the message to the AdeR via autophosphorylations to initiate the required response (34, 35). AdeR protein recognizes phosphorylated cytoplasmic domain of AdeS which becomes dimeric form. The binding of AdeR to phosphorylated AdeS results in the phosphoryl transfer from AdeS to aspartate residue of AdeR for its activation. The activated AdeR functions as transcription factor for turning on the other genes involved in efflux pump.

The TCSs also allows antibiotics to be transported through the cell membrane to the outside of the cell. Unlike bacteria with a single-component system, which transports antibiotics only to the periplasm, bacteria with a TCSs are more antibiotic resistant than bacteria with single-component system (1, 14, 24).

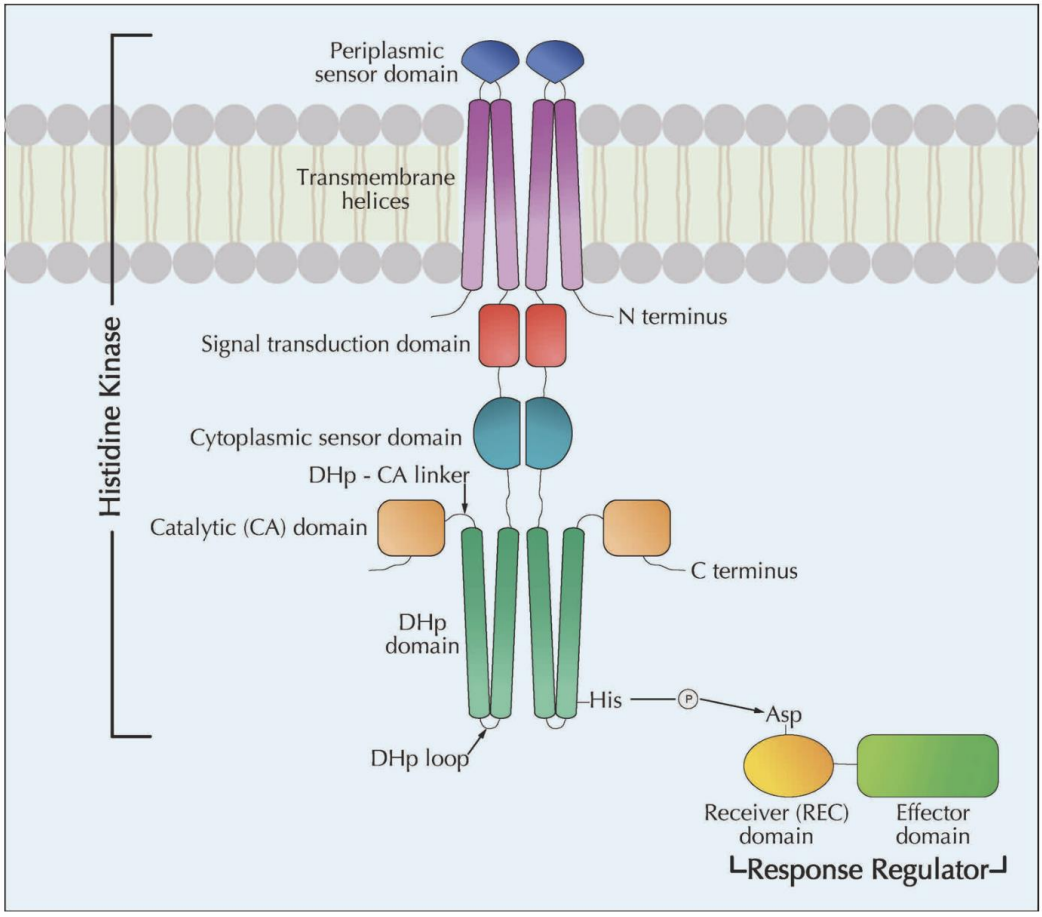

Figure 4. Two-component regulatory system

Schematic diagram of cellular architecture of a typical two-component regulatory system as well the mechanism of phosphotransfer between two components (24).

Investigation of the protein structures

Structure of Response regulator (AdeR)

AdeR is a response regulator that consists of two domains; the receiver (REC) domain at the N-terminus, which activates the AdeR and the effector domain or DNA binding domain at the C-terminus, which binds to DNA as shown in figure 5. AdeR binds to direct-repeat DNA in the intercistronic region between *adeR* and *adeABC* (36).

Structure of Histidine kinase (AdeS)

AdeS consists of two N-terminal transmembrane of two subunits linked by a short extracellular sensor domain (residue 34-61), the HAMP domain (residue 84-138), the DHp (dimerization histidine phosphotransfer) domain (residue 146-204) that contains the histidine residues, and a C-terminal contains catalytic ATP (CA) (residue 204-357). When the DHp domain and CA domain are combined, it phosphorylates histidine residue to initiate the AdeS auto-phosphorylation. Then phosphoryl groups from the H-box are transferred to the aspartate residue in the receiver domain (REC) leading to AdeR activation as shown in figure 5 (37, 38).

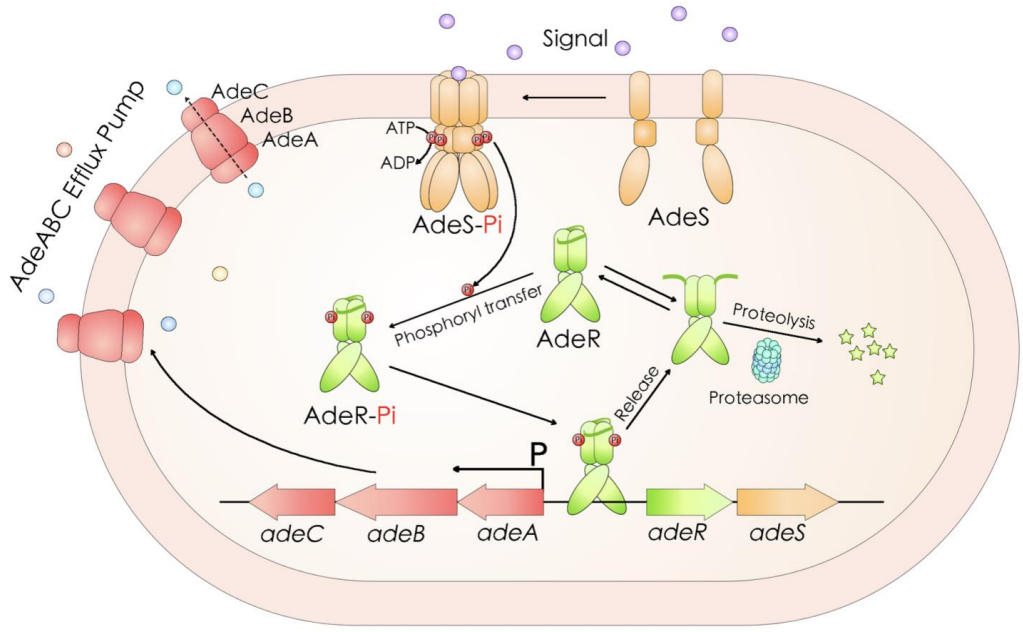

Figure 5. Two-component regulatory system

Working model of the AdeRS two component regulatory system in *A. baumannii* (37).

CHAPTER IV

METHODOLOGY

Conceptual framework

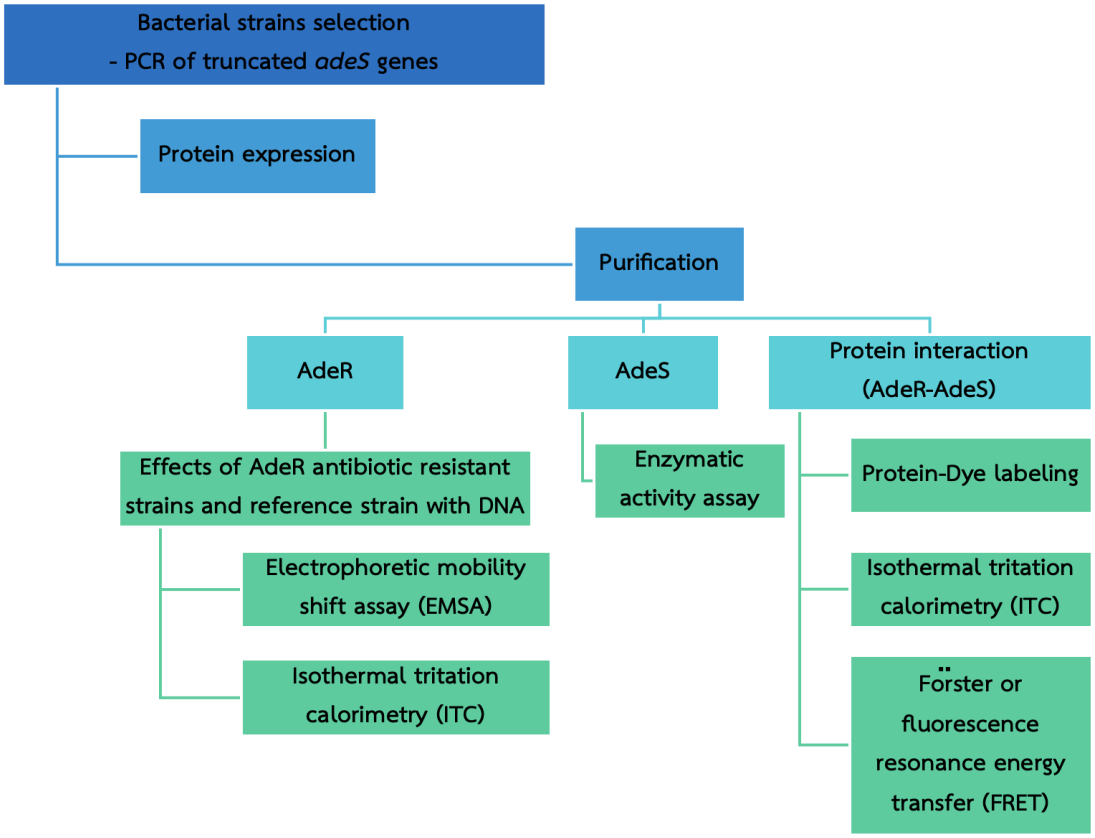

CHAPTER V

MATERIALS AND METHODS

Bacterials strains selection

Clinical isolates of antibiotic resistant *A. baumannii* (H1074 and G560) were selected from Department of Central Laboratory and Blood Bank, Faculty of Medicine in Vajira Hospital of Navamindradhiraj University, Thailand, and reference strain was *A. baumannii* ATCC19606. In H1074 was isolated from the blood culture of patients exhibiting antibiotic resistance. Interestingly, when an efflux pump inhibitor was administered, it led to a significant decrease in the minimum inhibitory concentration (MIC). This observation highlighted the potential involvement of H1074 in the functioning of the efflux pump. Similarly, G560 was isolated from a patient's urine sample exhibiting antibiotic resistance. Notably, G560 possessed an altered amino acid sequence in the DNA binding domain. This particular characteristic prompted its selection for the experiment, as it presented an opportunity to explore the implications of antibiotic resistant.

Construction of expression vectors for AdeR and AdeS

The amplified gene of adeR and adeS was constructed into expression in pET-22b+ containing C-terminal histidine tag using restriction site of 5' *Nde*I and 3' *Xho*I. The amplification cycling conditions were as follows: 30 cycles of denaturation at 98 °C for 30 seconds, annealing at 50 °C for 1 minute, and extension at 72 °C for 1 minutes. The PCR product was purified by Favorprep™ GEL/PCR Purification Mini Kit (Favorgen Biotech corp.) following by the manual protocol. Purified PCR product was digested with *Nde*I and *Xho*I and ligated with *NdeI/XhoI* digested pET-22b+ vector. The ligation mixture was transformed into *E. coli* ECOS.

DNA primers for N-terminal truncation of *adeS* gene

Table 2. Primers for truncated AdeS.

The sequences of primers for *A. baumannii* ATCC19606 (reference strain)	
Forward primer	5’ GGA ATT CCA TAT GAA GCG TTT CAT CGT GCC GAT TAA C 3’
Reverse primer	5’ CCG CTC GAG GTT GTT CAT GCT AAT TTT GAT GGT AAA AAC 3’
The sequences of primers for *A. baumannii* H1074 (antibiotic resistant strain)	
Forward primer	5’ GGA ATT CCA TAT GAA GCG TTT TAT TGT G 3’
Reverse primer	5’ CCG CTC GAG GTT ATT CAT AGA AAT 3’
The sequences of primers for *A. baumannii* G560 (antibiotic resistant strain)	
Forward primer	5’ GGA ATT CCA TAT GAA GCG TTT TAT TGT G 3’
Reverse primer	5’ CCG CTC GAG GTT ATT CAT AGA AAT 3’

DNA primers for *adeR* gene

Table 3. Primers for AdeR.

The sequences of primers for *A. baumannii* G560 (antibiotic resistant strain)	
Forward primer	5’ GGA ATT CCA TAT GAT GTT TGA TCA TTC T 3’
Reverse primer	5’ CCG CTC GAG GGC GTC ATC TTT TAC 3’

Protein expression

Expression vectors (pET-22b+) containing the *adeR* or *adeS* gene were transferred into host cells the ECOS™ *E. Coli* DE3 (Yeastern Biotech Co., Ltd.) using calcium chloride. The transformed cells were selected on LB agar containing 20 µg/ml ampicillin. The colony of transformed cells was inoculated in 50 ml of starting media for auto-induction (in 250 ml Erlenmeyer flask) containing ampicillin as a starting culture. The starting culture was incubated at 37 °C overnight in an incubator shaker (Unimax 1010 & Incubator 1000) (Heidolph, Germany) for overnight (12-14 hours). The overnight culture was inoculated into 1 L of auto-induction media in the 2.5 × 3 L Fernbach flask. The large-scale culture was incubated in a multitron incubator with orbital shaker (INFORS HT Multitron, Switzerland) at 37 °C for ~3 hours or optical density at 600 nm was ~1. Then the temperature of the incubator decreased to be 25 °C for protein expression. The large-scale culture was left overnight (~18 hours). The cells were harvested and kept at -80 °C until use.

Purification of AdeR

The frozen cell pellet was resuspended in 50 mM sodium phosphate pH 7.0, 300 mM NaCl and 80 mM imidazole and was disrupted using ultrasonic sonicator VCX750 (Sonics & Materials, USA) with an energy of 75 Amps, 6 s pulse on and 10 s pulse off. The suspension was kept on ice during sonication. The resulting cell debris suspension was centrifuged by Allegra™ 64R Centrifuge (Beckman Coulter, USA) at 18,000 rpm for 1 hr at 4 °C to collect the supernatant. The supernatant was purified with immobilized metal ion affinity chromatography using IMAC Sepharose™ (GE Healthcare, USA) (2.5 ϕ × 15 cm). Unbound proteins were removed using 50 mM sodium phosphate buffer pH 7.0, 300 mM NaCl and 80 mM imidazole 500 mL. AdeR fraction was eluted with the same buffer containing higher imidazole concentration of 300 mM. The purification procedure was performed at 4 °C. Fractions containing AdeR were identified by sodium dodecyl sulfate-polyacrylamide gel electrophoresis (SDS-PAGE). The eluted AdeR was concentrated using ultrafiltration using Amicon® stirred cell device (Merck, Germany) with a molecular mass cutoff of 10 kDa to

decrease solution volume to be ~5 mL. The filtration was performed under high pressure nitrogen gas of 50 Psi at 4 °C. The concentrated AdeR was exchanged in, and PD-10 column equilibrated with 50 mM sodium phosphate buffer pH 7.0 and 300 mM NaCl for removal of imidazole. The concentration of protein was determined using an extinction coefficient at 280 nm of 14.56 × 10^3 $M^{-1}cm^{-1}$.

Purification of AdeS

The frozen cell pellet was resuspended in 50 mM sodium phosphate pH 7.0, 300 mM NaCl and 80 mM imidazole and was disrupted using ultrasonic sonicator VCX750 (Sonics & Materials, USA) with an energy of 75 Amps, 6 s pulse on and 10 s pulse off. The suspension was kept on ice during sonication. The resulting cell debris suspension was centrifuged by Allegra™ 64R Centrifuge (Beckman Coulter, USA) at 18,000 rpm for 1 hr at 4 °C to collect the supernatant. The supernatant was purified with immobilized metal ion affinity chromatography using IMAC Sepharose™ (GE Healthcare, USA) (2.5 ϕ × 15 cm). Unbound proteins were removed using 50 mM sodium phosphate pH 7.0, 300 mM NaCl and 80 mM imidazole 500 mL. AdeS fraction was eluted with the same buffer containing higher imidazole concentration of 250 mM. The purification procedure was performed at 4 °C. Fractions containing AdeR were identified by sodium dodecyl sulfate-polyacrylamide gel electrophoresis (SDS-PAGE). The eluted AdeS was concentrated using ultrafiltration: Amicon® stirred cell device (Merck, Germany) with a molecular mass cutoff of 10 kDa, to decrease solution volume to be ~5 mL. The filtration was performed under high pressure nitrogen gas of 50 Psi at 4 °C. The concentrated AdeS was exchanged in, and PD-10 column equilibrated with 50 mM sodium phosphate buffer pH 7.0 and 300 mM NaCl for removal of imidazole. The concentration of protein was determined using an extinction coefficient at 280 nm of 19.94 × 10^3 $M^{-1}cm^{-1}$.

Measured the size of the protein using Fast protein liquid Chromatography

Fast protein liquid chromatography is a high capacity for analysis using ÄKTA pure 25 M1 (Cytiva, US). The stationary phase was Sephacryl™ S-200 High Resolution and equilibrated with 50 mM potassium phosphate containing 300 mM NaCl, pH 7.0 with flow rate of 0.5 ml/min and eluted with the same buffer at room temperature. The eluents were monitored at 280 and 620 nm using a UV-absorption detector for protein and baseline, respectively. The molecular weight was determined using standard calibration curve obtained from Gel filtration Calibration Kit HMW (Ovalbumin: 43 kDa, Conalbumin: 75 kDa, Aldolase: 158 kDa, Ferritin: 440 kDa, Blue Dextran 2000: > 2000 kDa). Void volume of the column was determined from the blue dextran elution volume. The protein standard includes 4 mg/mL Aldolase, 0.3 mg/mL Ferritin, 3 mg/mL Conalbumin, and 10 mg/mL blue dextran. (39, 40).

Preparation of DNA for AdeR binding

AdeR proteins are mixed with intercistronic (as underline) DNA 129 bp (5' TTT TGA TGT TCG TAT TAT TTT TGA TGA GTG TGT AGG GAT AAT CAC TAA AGT GTG GAG TAA GTG TGG AGA AAT ACG GAT AAT TTA GCG TAT GAT GAG TTG AAG CAC TTT CTA TAG CCA GAT TAT CTA TGT 3').

Primers for amplified double strand DNA probe (intercistronic DNA)

Forward primer = IntercadeR_N_F (5’ AAA ACT ACA AGC 3’) and

Reverse primer = IntercadeR_N_R (5’ ACA TAG ATA ATC 3’)

The amplification cycling conditions were as follows: 30 cycles of denaturation at 98 °C for 30 seconds, annealing at 60 °C for 15 seconds, and extension at 72 °C for 1 minutes. The PCR product was purified by Favorprep™ GEL/PCR Purification Mini Kit (Favorgen Biotech corp.) following by the manual.

Electrophoretic mobility shift assay (EMSA)

EMSA is used to analyze interaction between proteins and double strand DNA using native Polyacrylamide Gel Electrophoresis (PAGE) to resolve protein-DNA complex from free DNA and free protein. The double strand DNA with size of 129 bp containing protein binding region of 25 bp with flank region at 5' and 3'. DNA bound protein migrate shorter distance compared with a free DNA probe. The binding reactions mixture with native AdeR as a reference and antibiotic resistant strains (20, 30, 40, 50, 60, 70 and 80 µM) and DNA (150 ng). The binding reactions were performed in 10 mM KH_2PO_4 pH 7.5, 50 mM KCl and 1 mM DTT. The reaction was incubated at room temperature (25 °C) for 30 minutes then analyzed using 8% native polyacrylamide gel containing 0.5 X Tris-borate buffer and 50% glycerol. Free DNA and protein bound DNA were detected using fluorescence dye (Visafe Red gel staining) on Gel Doc EZ Imager (Bio-Rad) (36, 41, 42).

Isothermal titration calorimetry (ITC)

All ITC experiments were carried out at 25 °C using a Microcal ITC200 calorimeter (GE Healthcare). Protein and DNA samples were mixed in appropriate buffers, such as 50 mM KH_2PO_4, and 300 mM NaCl pH 7.0. All ITC data were analyzed with the complementary Microcal ITC data analysis package under single binding site mode (36, 43-47).

The experiments will be divided into two categories: protein-DNA binding and protein-protein binding. The following experimental methods and conditions are specified for protein-DNA binding:

- A sample cell will be prepared with a concentration of 396 nM of AdeR ATCC19606. And DNA will be injected into the cell at a concentration of 3.96 nM, with 2 µl injected per time. The reference sample will consist of DI water. The experimental parameters include a temperature of 25°C, a reference power of 10 µcal/s, a stir speed of 500 rpm, an initial delay of 60 seconds, and a total of 13 injections.

- A sample cell will be prepared with a concentration of 83.02 μM of AdeR ATCC19606. And DNA will be injected into the cell at a concentration of 892.65 nM of DNA, with 2 μl injected per time. The reference sample will consist of DI water. The experimental parameters include a temperature of 25℃, a reference power of 10 μcal/s, a stir speed of 500 rpm, an initial delay of 60 seconds, and a total of 13 injections.

The following experimental methods and conditions are specified for protein-protein binding:

- A sample cell will be prepared with a concentration of 50 mM of KH_2PO_4 buffer. And buffer will be injected into the cell at a concentration of 50 mM of KH_2PO_4 buffer, with 2 μl injected per time. The reference sample will consist of DI water. The experimental parameters include a temperature of 25℃, a reference power of 10 μcal/s, a stir speed of 500 rpm, an initial delay of 60 seconds, and a total of 13 injections.
- A sample cell will be prepared with a concentration of 1 mM of AdeR ATCC19606. And AdeS ATCC19606 will be injected into the cell at a concentration of 10 μM of AdeS ATCC19606, with 2 μl injected per time. The reference sample will consist of DI water. The experimental parameters include a temperature of 25℃, a reference power of 10 μcal/s, a stir speed of 500 rpm, an initial delay of 60 seconds, and a total of 13 injections.

Enzymatic activity assay

ATP hydrolysis from kinase activity of histidine kinase

ATP hydrolysis activity was be determined by coupling the ADP production with pyruvate kinase (PK) and lactate dehydrogenase (LDH) systems. The ADP generated from kinase activity is changed to be ATP with production of pyruvate from phosphoenolpyruvate (PEP). The produced pyruvate is coupled with LDH and NAD^+ to form NADH of which the absorbance can be monitored at 340 nm. shown in figure 6 (37, 48).

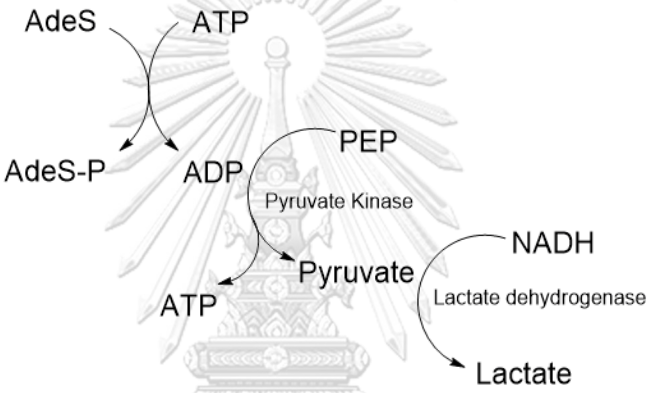

Figure 6. Coupling reaction for kinase activity assay.

Table 4. ATP hydrolysis from kinase activity assay

	Concentration	Volume (total volume = 1 ml)
ATP	400 µM	400 µl
PEP	400 µM	200 µl
Pyruvate kinase (PK)		4 µl
NADH	200 µM	200 µl
Lactate dehydrogenase (LDH)	10 mg/mL	40 µl
AdeS	20 µM	40 µl
Tris buffer pH 7.0		116 µl

Malachite green Phosphate Assay

The Malachite Green Phosphate Assay is based on the ability of phosphate ions to form a phosphomolybdate complex with ammonium molybdate under acidic conditions. This complex then reacts with malachite green to form a green-colored complex. The intensity of the green color is directly proportional to the concentration of phosphate ions present in the sample. The rapid color formation from the reaction can be conveniently measured on a spectrophotometer (600–660 nm). The quantification of phosphate released during a malachite green assay is determined using the assay phosphate standard. The following assay method is commonly used. Solution A is ammonium molybdate solution made by mixing 4.2% ammonium molybdate ($(NH_4)_6Mo_7O_{24}$) and 4 N HCl. Solution B is 0.045% Malachite green. (49-51).

Table 5. Phosphate standard curve

1 mM Phosphate standard (working stock) (µl)	Distilled water (µl)	Phosphate concentration (µM)
0	1000	0
10	990	10
20	980	20
30	970	30
40	960	40
50	950	50
60	940	60
70	930	70
80	920	80

Protein-dye labeling

The protein labeling with fluorescence dyes is employed for fluorescence resonance energy transfer (FRET) to investigate protein interaction between AdeR and AdeS. The dyes Cy3 and Cy5 used for FRET are mono-reactive NHS Esters (GE Healthcare) which can attach to proteins in the primary amine group. The proteins linked with dyes contain fluorescence properties which can be determined using spectrofluorometer (Shimadzu, JAPAN). The proteins labeling with dyes reactions were performed in 50 mM phosphate buffer pH 7.0. AdeR and AdeS will be attached to Cy3 and Cy5 dye respectively. The labelling reaction is an incubation at 25 °C for 3 hours and then is kept at 4 °C for about 16-18 hours (overnight). Excess dyes are removed using gel filtration (PD-10 column) (52).

Forster or fluorescence resonance energy transfer (FRET)

FRET is the process of transferring non-radiative energy between donor-acceptor pair. The emission intensity of donor from is transferred to the acceptor's ground state. FRET is also known as "fluorescence resonance energy transfer" when the donor and acceptor are both fluorophores are in suitable distance.

The requirement for selecting the donor and acceptor: 1) the donor-acceptor pair should be in close position (typically 1 – 10 nm.), 2) the donor emission spectra should overlap with the acceptor absorption or excitation spectra. Therefore, this technique can be used to investigate the Protein-protein interaction using the fluorescence signal. In this study, Cy3 dye will be used as the donor and Cy5 dye was used as the acceptor. Both donor and acceptor have their own excitation and emission, Cy3 dye has an excitation wavelength of 550 nm and an emission wavelength of 570 nm. Cy5 has an excitation wavelength of 649 nm and an emission wavelength of 670 nm. (52, 53).

CHAPTER VI

RESULTS

Protein purification and expression

1.1 Purification and expression of full-length AdeR (ATCC19606) and antibiotic resistant strains AdeR (H1074 and G560)

AdeR ATCC19606, H1074 and G560 were purified using IMAC) sepharose. The column was washed with buffer containing 80 mM imidazole without an expected size of 29 kDa of AdeR (W, in Figure 7A, 7B and 7C). The fraction of AdeR was eluted with buffer containing higher imidazole of 300 mM (E, in Figure 7A, 7B and 7C). The purity of protein higher than 90% purity was judged by SDS-PAGE with Coomassie Blue R staining. The yield expression of AdeR ATCC19606, AdeR H1074 and AdeR G560 were 0.54, 0.31 and 0.23 g/L, respectively. The analysis of native molecular weights using FPLC of AdeR ATCC19606, H1074 and G560 provided molecular mass of 57.92 kDa, 63.26 kDa and 63.69 kDa, respectively (Figure 9). The calculation of molecular weight of the subunit of AdeR ATCC19606, H1074 and G560 using amino acid sequences were 29.16 kDa, 29.22 kDa and 29.13 kDa. The results suggested that all native forms of AdeR were dimer, respectively (Figure 8 and 9).

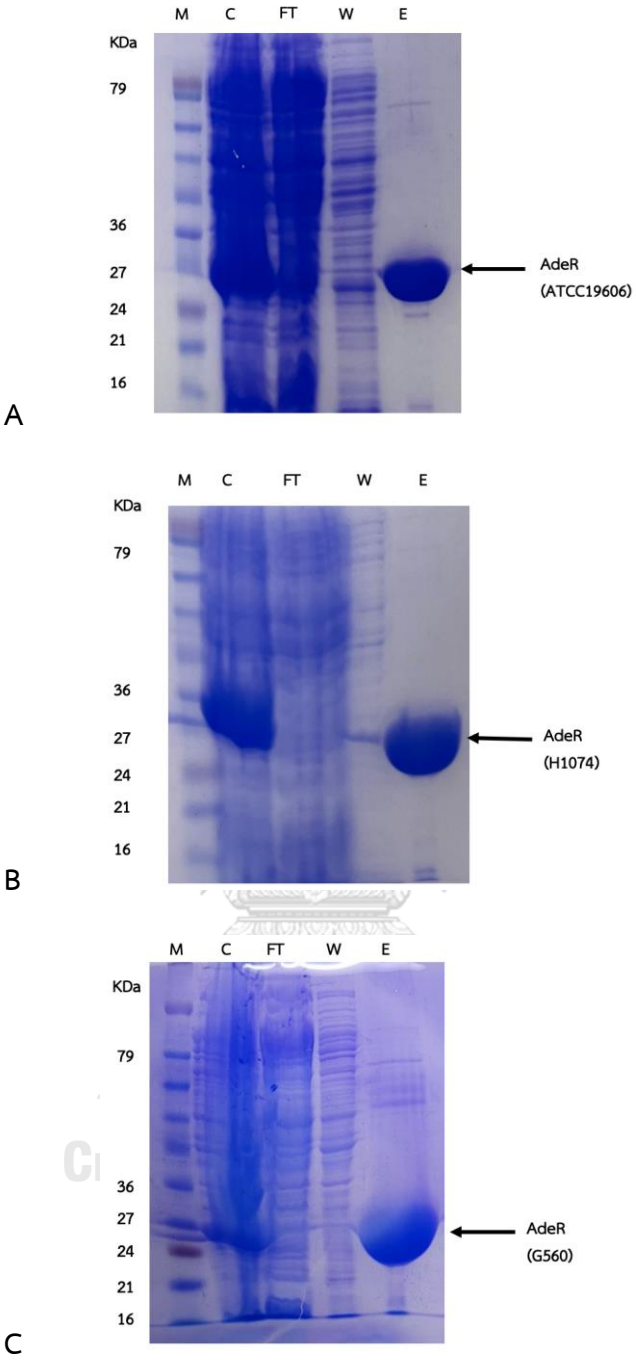

Figure 7. Protein expression and purification using IMAC sepharose.

The fractions from crude extract were run on SDS-PAGE according to M: marker, C: crude cell, FT: flow through, W: wash, and E: elution (A) Purification of AdeR ATCC19606. (B) Purification of AdeR H1074. (C) Purification of AdeR G560. The fractions were analyzed using 12% SDS-PAGE.

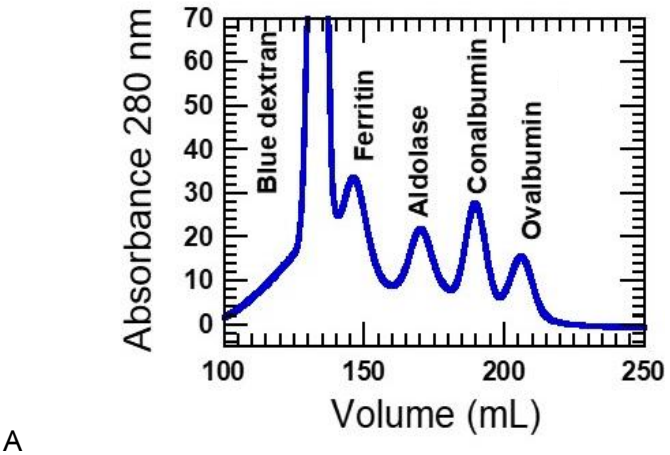

A

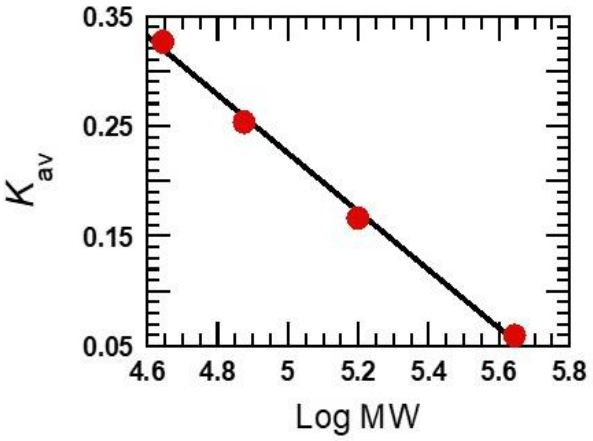

B

Figure 8. The chromatogram of standard protein molecular weights.

(A) The linear equation of the calibration curve incorporates four proteins: ferritin, aldolase, conalbumin, and ovalbumin, along with blue dextran. (B) The calibration curve of plot partition coefficient (K_{av}) of protein molecular weights and versus log MW. Chromatography is utilized to determine the molecular weight and size of proteins. Blue dextran is the first protein to be eluted from the column, followed by ferritin, aldolase, conalbumin, and ovalbumin, respectively.

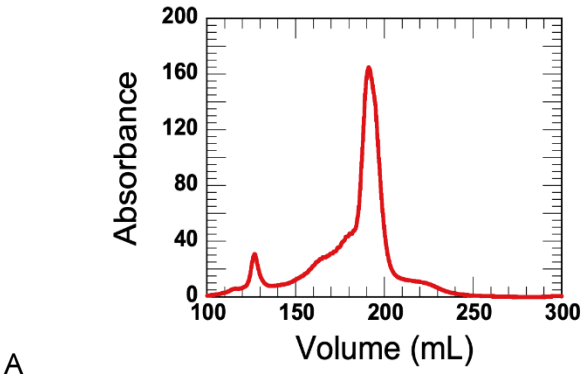

A

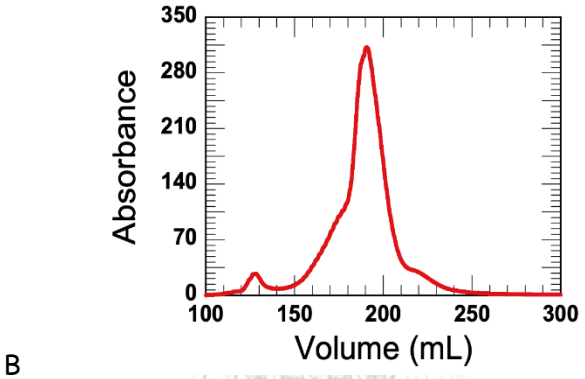

B

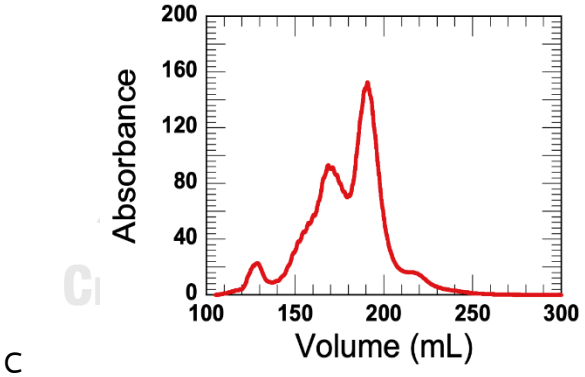

C

Figure 9. Determination native form of AdeR

The chromatogram of AdeR ATCC19606 (A), AdeR H1074 (B), and AdeR G560 (C) used for determination of the protein molecular weight.

1.2 Purification and expression of truncated AdeS (ATCC19606) and antibiotic resistant strains AdeS (H1074 and G560)

AdeS ATCC19606, H1074 and G560 were purified using immobilized IMAC sepharose. The column was washed with buffer containing 80 mM imidazole without expected size of AdeS of 32 kDa (W, in Figure 10A, 10B, and 10D). The fraction of AdeS was eluted with buffer containing higher imidazole of 250 mM (E, Figure 10A, 10B, and 10D). The purity of protein higher than 90% purity was judged by SDS-PAGE with Coomassie Blue R staining. The yield expression of AdeS ATCC19606, AdeS H1074 and AdeS G560 were 0.59, 0.19 and 0.20 g/L. The analysis of native molecular weights using FPLC equipped with size-exclusion chromatography of AdeS ATCC19606, H1074 and G560 provided molecular mass of 75.69 kDa, 89.84 kDa and 59.17 kDa, respectively (Figure 11). The calculation of molecular weight of the subunit of AdeS ATCC19606, H1074 and G560 using amino acid sequences were 31.65 kDa, 31.82 kDa and 31.71 kDa. The results suggested that all native form of AdeS were dimer (Figure 8 and 11).

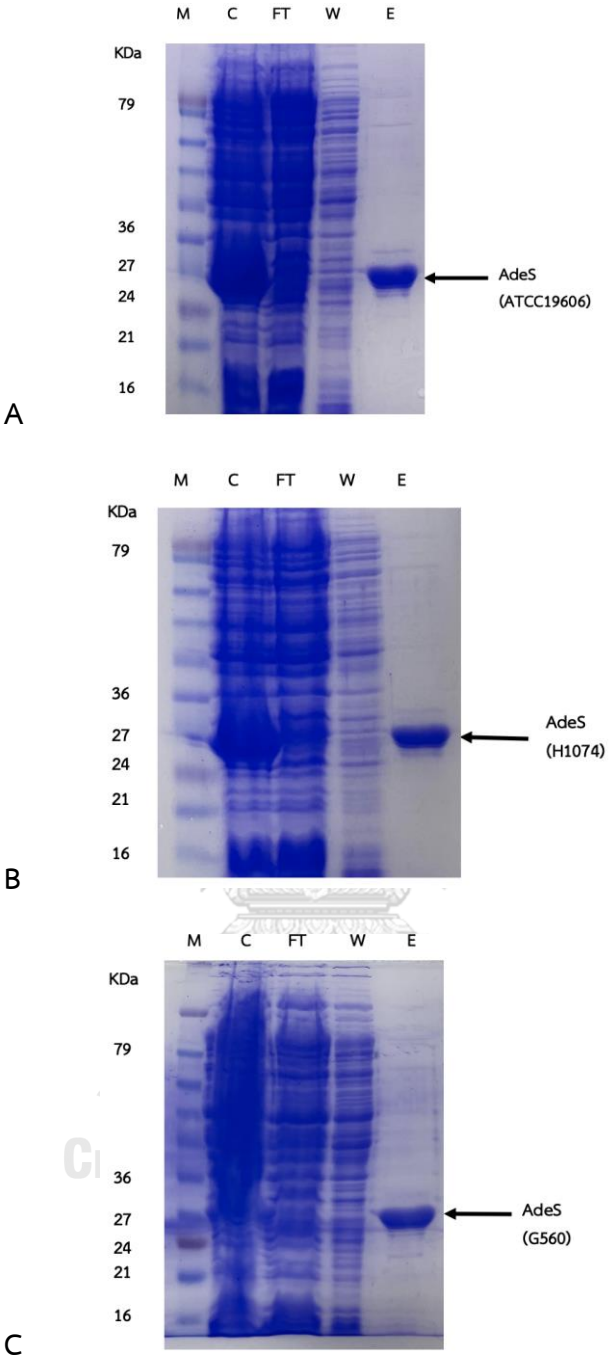

Figure 10. Protein expression and purification using IMAC sepharose.

The fractions from crude extract were run onSDS-PAGE according to M: marker, C: crude cell, FT: Flow through, W: wash, and E: elution (A) Purification of AdeS ATCC19606. (B) Purification of AdeS H1074. (C) Purification of AdeS G560. The fractions were analyzed using 12% SDS-PAGE.

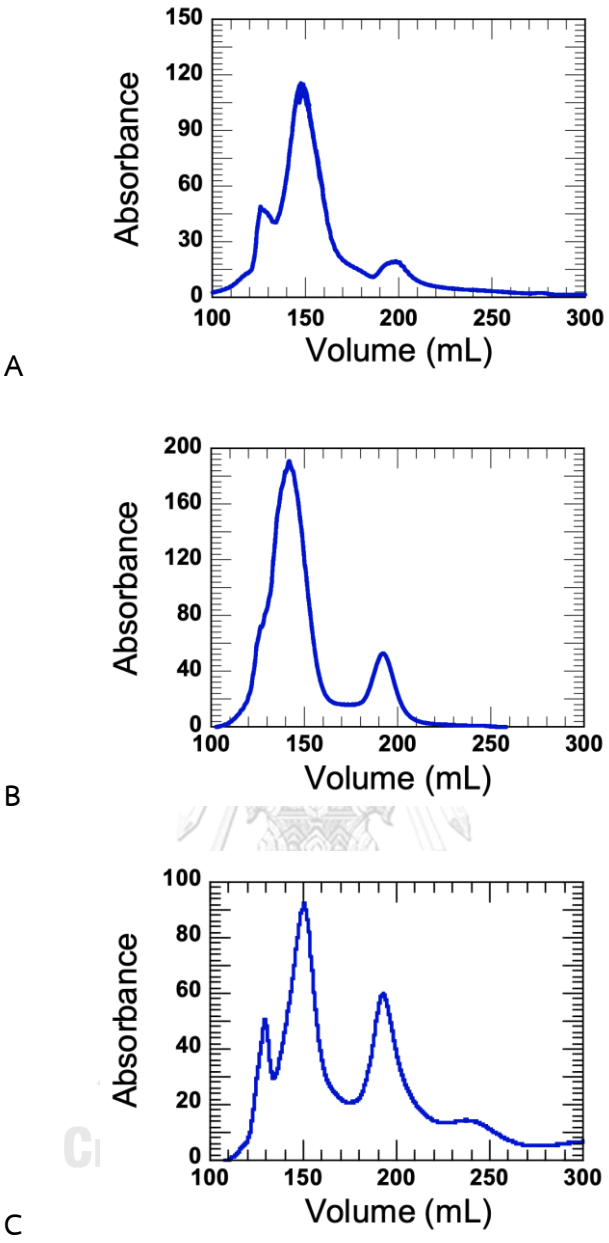

Figure 11. Determination native form of AdeS

The chromatogram of AdeS ATCC19606 (A), AdeS H1074 (B), and AdeS G560 (C) used for determination of the protein molecular weight.

Investigation of the interaction of AdeR and DNA using EMSA and ITC

Electrophoretic mobility shift assay (EMSA) of AdeR-DNA complex

EMSA was used to analyze interaction between proteins and double strand DNA using native polyacrylamide gel electrophoresis (PAGE) to resolve protein-DNA complex from free DNA and free proteins. AdeR binds to double strand DNA in the region of 25 bp. DNA bound protein migrates shorter distance compared with a free DNA probe. The results of EMSA showed all antibiotic resistant strains bound with DNA similar to the reference strain as shown in Figure. 12A, 12B, 12C, 12D, 12E, and 12F.

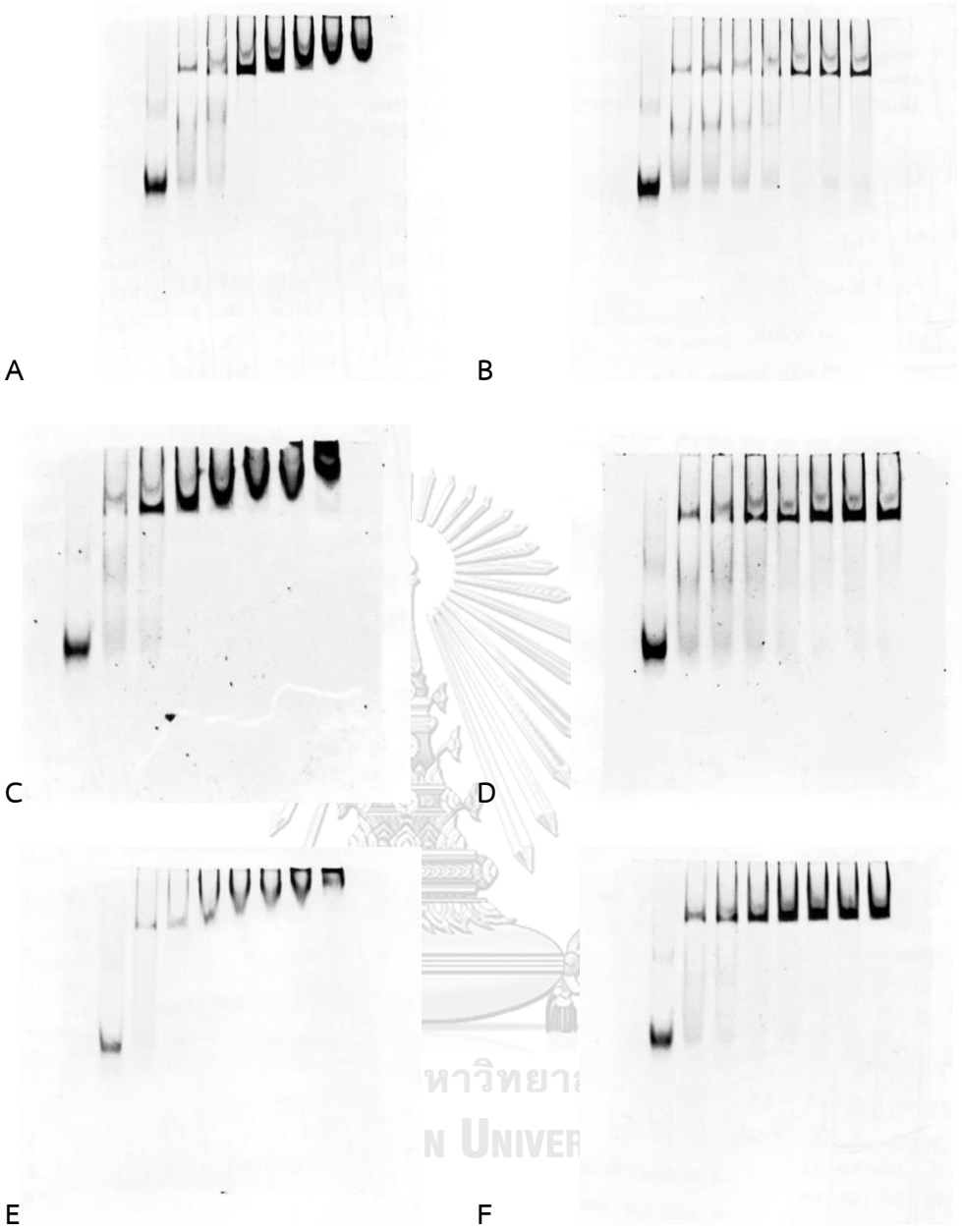

Figure 12. The EMSA results of the binding of DNA with AdeR ATCC19606 reference strain and antibiotic resistant strain H1074 and G560 on the intercistronic region.

The protein-DNA complex was analyzed on 8% native polyacrylamide gel and stained by Visafe red gel staining. Each lane is represented the varied AdeR concentrations (from left to right) and fixed DNA of 150 ng: in left figures (A, C, and E) lane 1; DNA, lane 2; 20 μM, lane 3; 40 μM, lane 4; 80 μM, lane 5; 160 μM, lane 6; 320 μM, lane 7; 640 μM, and lane 8; 1,280 μM and in right figures (B, D, and F) lane 1;

DNA, lane 2; 20 μM, lane 3; 30 μM, lane 4; 40 μM, lane 5; 50 μM, lane 6; 60 μM, lane 7; 70 μM, and lane 8; 80 μM. (A and B) The EMSA of AdeR reference strain (ATCC19606) proteins. (B and C) The EMSA of AdeR antibiotic resistant strain (H1074) proteins. (E and F) The EMSA of AdeR antibiotic resistant strain (G560) proteins.

Isothermal titration calorimetry (ITC) of AdeR-DNA complex

A slight binding between AdeR and DNA was detected with the use of 3.96 nM DNA and 396 nM AdeR ATCC19606, resulting in a K_d value of 0.00303 ± 0.431 nM. The corresponding enthalpy change (ΔH) was measured as 7.35 ± 3640 kcal/mol, while the Gibbs free energy change (ΔG) was found to be -3.44 kcal/mol. Additionally, the value of -TΔS was determined to be -10.8 kcal/mol, as illustrated in Figure 13.

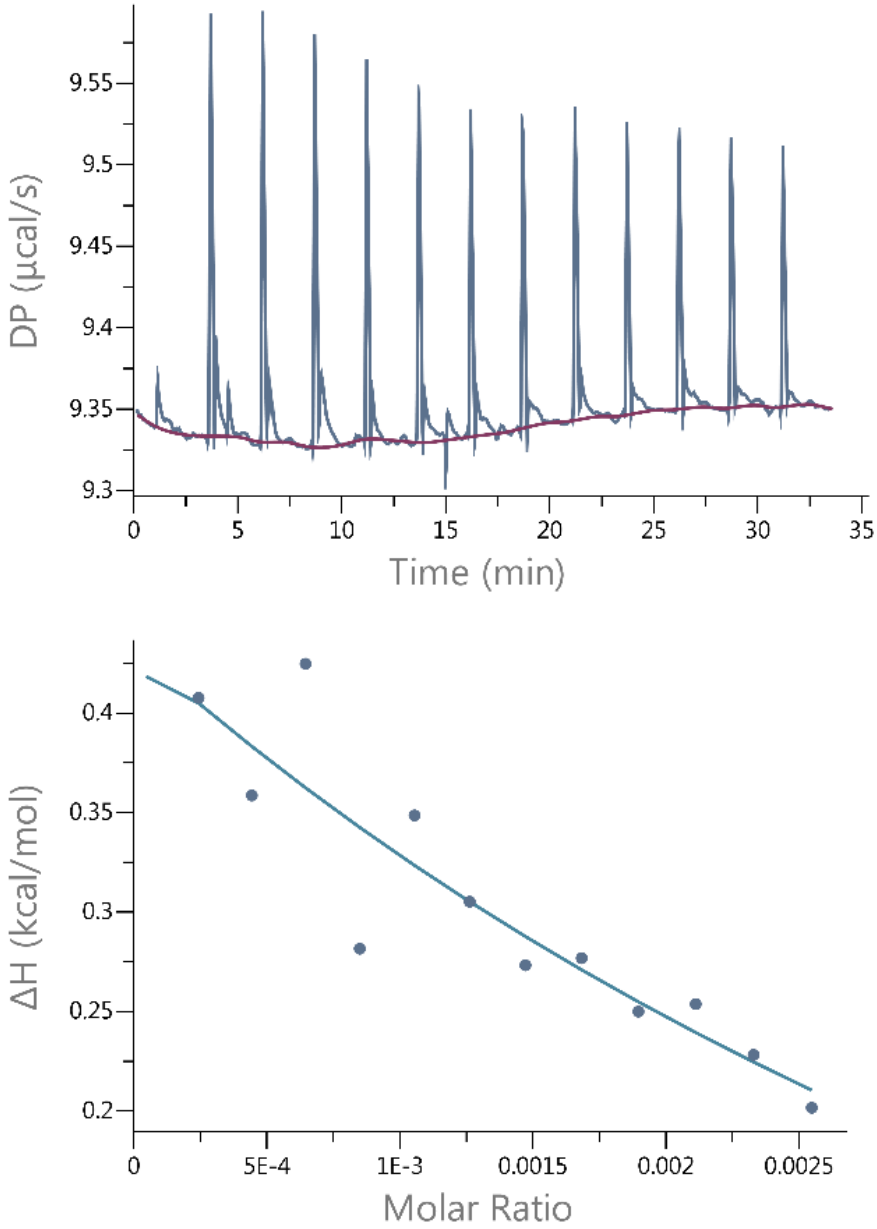

Figure 13. Isothermal titration calorimetry of AdeR ATCC19606 to 3.96 nM of DNA

When the concentration of AdeR ATCC19606 was increased to be 83.02 µM with 892.65 nM of DNA, no binding was observed, as shown in Figure 14.

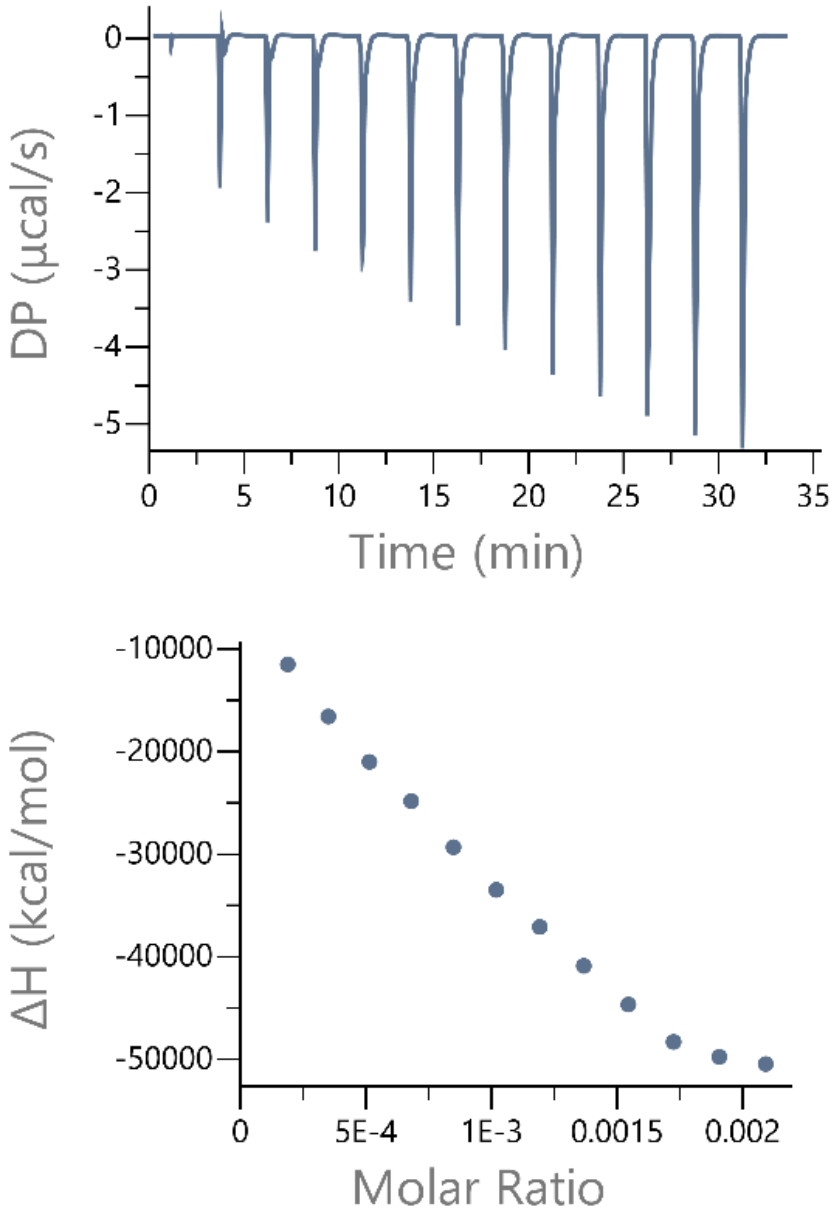

Figure 14. Isothermal titration calorimetry of AdeR ATCC19606 to 892.65 nM of DNA

Based on the information presented in Figure 13 and 14, there was no conclusion for binding between DNA and AdeR ATCC19606. The EMSA experiments confirmed binding of DNA and AdeR. The ITC experimental conditions may be figured out in the future.

Investigation of the interaction between AdeR and AdeS using FRET

FRET is the process of transferring energy between donor-acceptor pair. The emission intensity of donor is transferred to the acceptor's ground state. FRET is also known as “fluorescence resonance energy transfer” when the donor and acceptor are both fluorophores and in suitable distance.

The requirements for donor and acceptor selection are: 1) the donor-acceptor pair should be in close position (typically in range of 1 – 10 nm.), 2) the donor emission spectra should overlap with the acceptor absorption or excitation spectra.

To study of protein interactions between AdeR (ATCC19606) and AdeS (ATCC19606), the experiments were set up using AdeR as a donor using Cy3 dye and AdeS as acceptor using Cy5 dye. The emission spectrum of AdeR labeled with Cy3 was from excitation at wavelength of 549 nm has overlap region of 620 – 680 nm. For FRET analysis, the wavelength of 485 nm was chosen for excitation that shown in Figure 15. A FRET signal can be generated by combining 1 μM Cy3-labeled AdeR (ATCC19606) and 1 μM Cy5-labeled AdeS (ATCC19606) and exciting them at 485 nm, as shown in Figure 16.

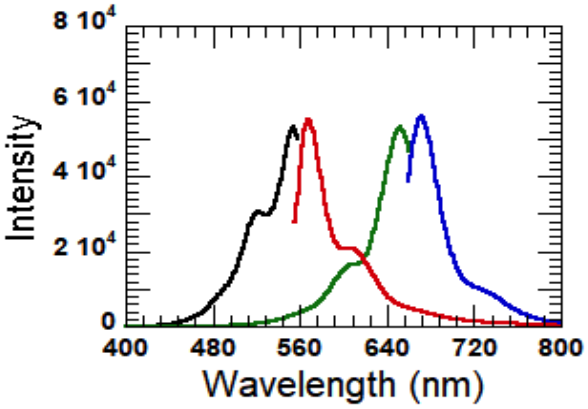

Figure 15. Excitation and emission spectra of AdeR (ATCC19606) labeled with Cy3 and AdeS (ATCC19606) labeled with Cy5.

The excitation and emission spectrum of AdeR labeled with Cy3 shown in left peaks (black line and red line), and AdeS labeled with Cy5 shown in right peaks (green line and blue line), respectively.

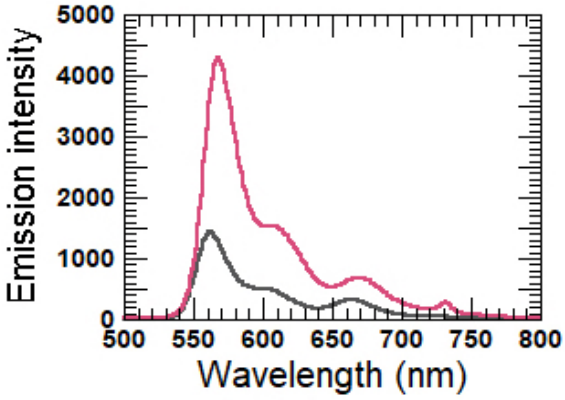

Figure 16. Emission spectra of FRET from interaction between AdeR-Cy3 (ATCC19606) and AdeS-Cy5 (ATCC19606).

The emission spectrum was excited at 485 nm. Black line is the solution mixture of 1 μM Cy3 and 1 μM Cy5. Pink line is mixed with 1 μM AdeR-Cy3 and 1 μM AdeS-Cy5.

The FRET titration experiment was performed by increasing the concentration of the acceptor fluorophore while keeping the donor fluorophore concentration constant. The fluorescence emission spectra were recorded at each titration point. FRET efficiency and interactions were analyzed. When attempting a titration to investigate protein interactions and evaluate the fluorescence signal of Cy5 upon excitation of Cy3, the control group was subjected to the following conditions.

1. control; 1 μM Cy3 titrated with Cy5
2. 1 μM AdeR-Cy3 titrated with AdeS-Cy5
3. 1 μM Cy3 titrated with AdeS-Cy5
4. 1 μM AdeR-Cy3 titrated with Cy5

It was observed that a FRET signal was detected, as illustrated in Figure 17 and 18. The emission spectrum of Cy5 exhibited a noticeable reduction in intensity in the presence of the donor, while simultaneously transmitting this signal to the acceptor, resulting in an increase in intensity over time.

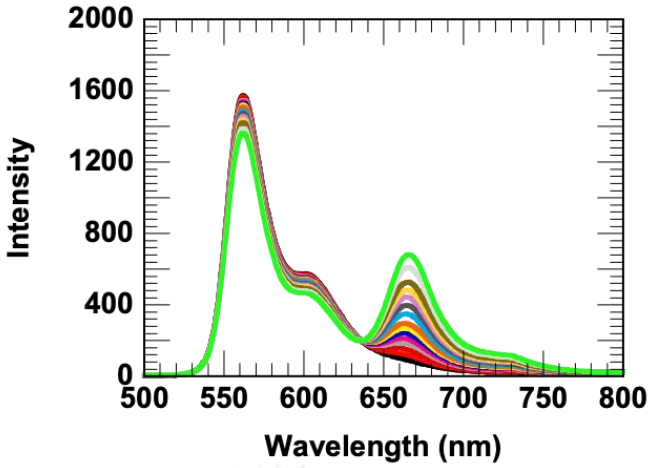

Figure 17. 1 μM Cy3 titrated with Cy5

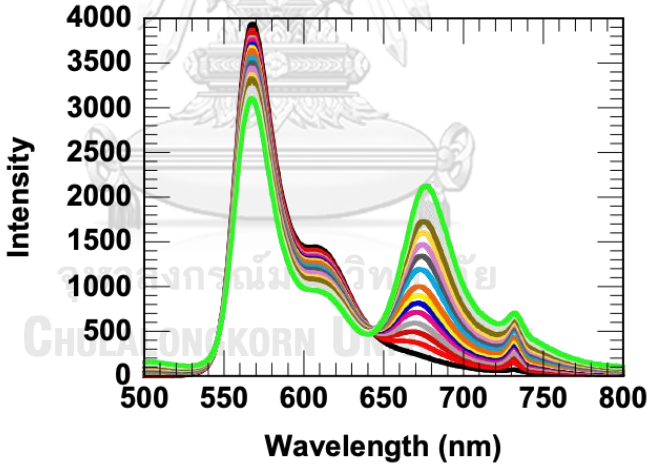

Figure 18. 1 μM AdeR-Cy3 (ATCC19606) titrated with AdeS-Cy5 (ATCC19606)

However, upon analyzing Figures 19 and 20, it is evident that a FRET signal was not actually generated. In Figure 19, when using 1 μM Cy3 titrated with AdeS-Cy5, there was no decrease in the signal from the donor; instead, there was an increase in the intensity of the acceptor. Similarly, in Figure 20, when using 1 μM AdeR-Cy3 titrated with Cy5, there was only a slight increase in acceptor intensity. This indicates that whether or not AdeR is bound to the donor Cy3, it fails to effectively transmit the signal to the acceptor. The observed increase in acceptor intensity is more likely due to other factors, rather than a genuine FRET signal. This finding is further supported by Figures 19, 20, and 21.

In Figure 21, we plotted graphs representing the relationship between increasing intensity and concentration. Our expectation was that if a FRET signal were indeed generated from the interaction between AdeR and AdeS, the blue dotted line (Cy3 titrated with AdeS-Cy5) should not closely resemble the red dotted line (AdeR-Cy3 titrated with AdeS-Cy5), as there would be no protein bound to Cy3 in the former case. Instead, it should align closely with the black dotted line (Cy3 titrated with Cy5) and the green dotted line (AdeR-Cy3 titrated with Cy5). Thus, it can be concluded that the interaction between AdeR and AdeS cannot be identified based on the results presented in Figure 21.

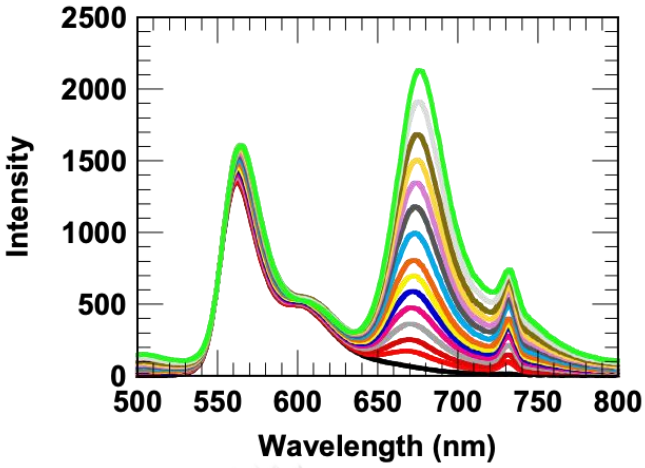

Figure 19. 1 μM Cy3 titrated with AdeS-Cy5 (ATCC19606)

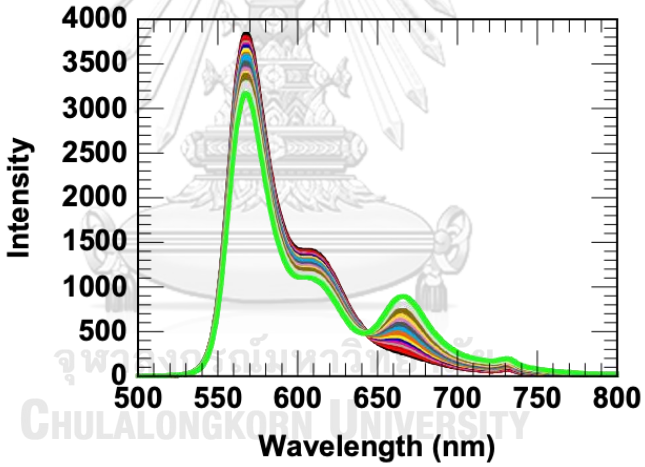

Figure 20. 1 μM AdeR-Cy3 (ATCC19606) titrated with Cy5

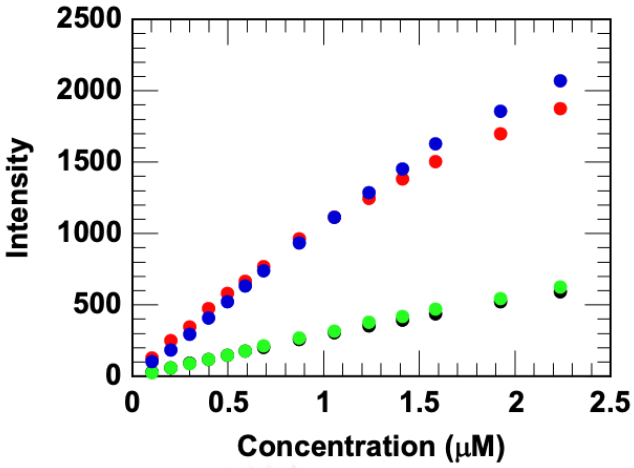

Figure 21. Plot a graph illustrating the correlation between concentration and intensity.

The black dotted line represented the titration of Cy3 with Cy5, the green dotted line represented the titration of AdeR-Cy3 with Cy5, the blue dotted line represented the titration of Cy3 with AdeS-Cy5. The red dotted line represented the titration of AdeR-Cy3 with AdeS-Cy5.

Kinase activity assay of AdeS

The test was classified into two different categories: 1. Malachite green phosphate assay and 2. Coupling assay.

In the Malachite green phosphate assay, it was observed that neither the reference strain (ATCC19606) nor the antibiotic resistant strains (H1074 and G560) released any phosphate, and compared to the Phosphate standard curve (Figures 22, 23, 24, and 25) and the result of Enzymatic activity assay (Coupling assay). This method utilizes a kinetic approach to examine the activity of enzymes or the AdeS protein. When ATP hydrolysis activity can be determined by coupling the ADP production with pyruvate kinase (PK) and lactate dehydrogenase (LDH) systems. The ADP generated from kinase activity is changed to be ATP with production of pyruvate from phosphoenolpyruvate (PEP). The produced pyruvate is coupled with LDH and NAD^+ to form NADH of which the absorbance can be monitored at 340 nm. The initial rates were measured as follows: The reference strain (AdeS ATCC19606) demonstrated a rate of 0.0139 μM/s, whereas the antibiotic resistant strains (AdeS H1074 and AdeS G560) exhibited rates of 0.0416 μM/s and 0.0372 μM/s, respectively. Consequently, it can be concluded that AdeS acts as a histidine kinase. Moreover, the coupling assay revealed that the presence of AdeR did not induce any notable changes or disturbances in the activity of AdeS, specifically in terms of phosphate binding.

Table 6. Results of enzymatic activity assay (coupling assay)

	Initial rate (μM/s)
AdeS ATCC19606	0.0139
AdeS H1074	0.0416
AdeS G560	0.0372
AdeS + AdeR (ATCC19606)	0.0702
AdeS + AdeR (H1074)	0.1264
AdeS + AdeR(G560)	0.1314

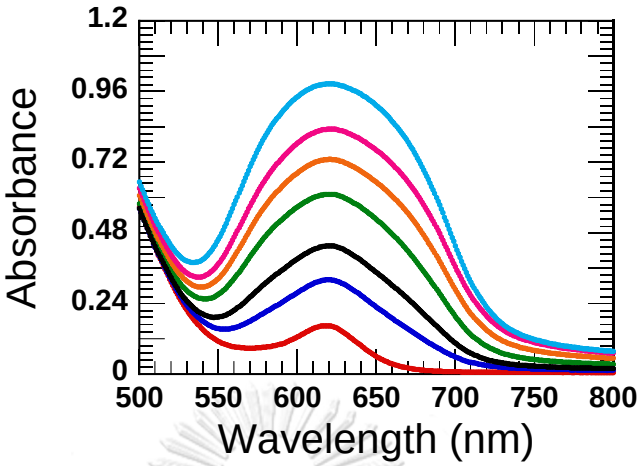

Figure 22. Spectrum of the Phosphate standard

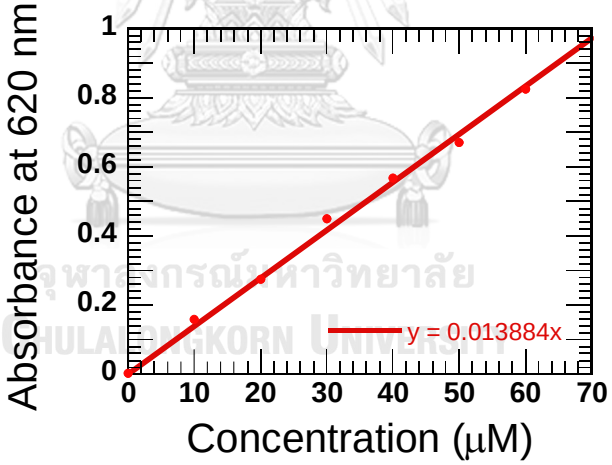

Figure 23. Standard Curve of Phosphate Standard

The figure presents the standard curve depicting the relationship between various concentrations of the Phosphate standard, ranging from 10 to 80 μM.

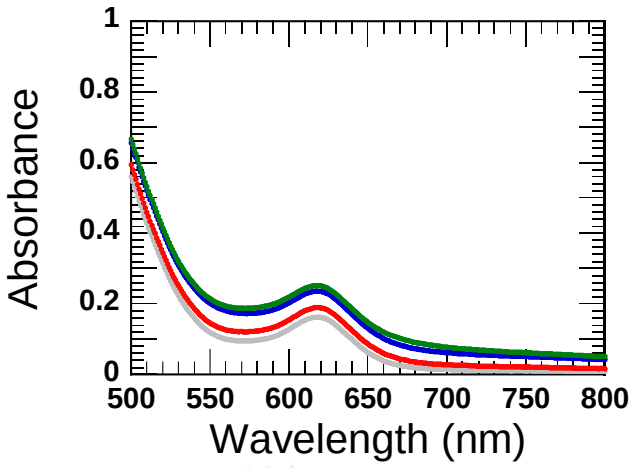

Figure 24. Spectrum of the Malachite Green used for Phosphate assay of AdeS.
The red line represents AdeS ATCC19606, the green line represents AdeS G560, and the blue line represents AdeS H1074.

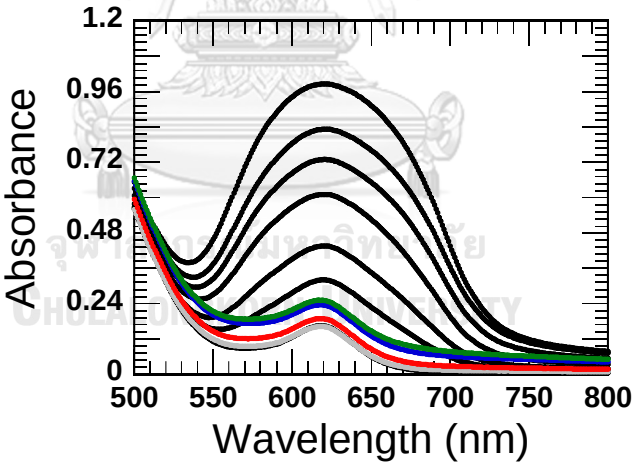

Figure 25. Spectrum of the Resulting Phosphate by Comparing Phosphate Standards (10 – 80 µM) and AdeS.
The red line represents AdeS ATCC 19606, the blue line represents AdeS H1074, and the green line represents AdeS G560.

Investigation of Protein-Protein Interactions using Isothermal Titration Calorimetry

This study focuses on investigating protein-protein interactions by analyzing binding values using isothermal titration calorimetry.

As indicated in the figure 26, the chromatogram obtained from the control sample (buffer-to-buffer interaction) does not align with the anticipated results. Consequently, it is not possible to proceed with further experiments to investigate the binding between AdeR and AdeS.

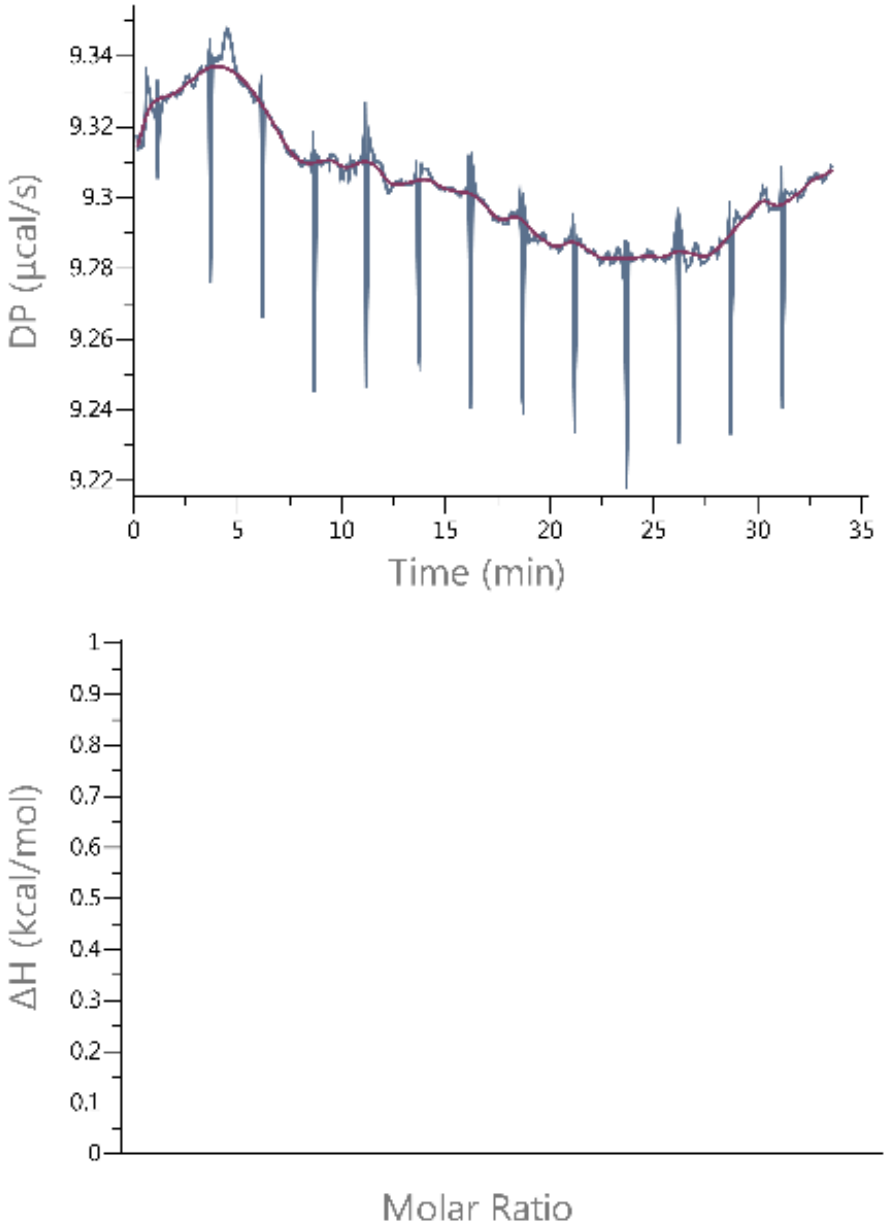

Figure 26. Isothermal titration calorimetry of buffer to buffer

CHAPTER VII

DISCUSSION

A. baumannii is a major cause of nosocomial infections, particularly in ICU patients. The emergence of multiple drug-resistant *A. baumannii* (MDRAB) has become a global concern, as it limits the effectiveness of antimicrobial treatments (1, 3, 6, 7). The AdeABC efflux pump, belonging to the resistance-nodulation cell division (RND) family, was identified in 2001 and is strongly associated with antimicrobial resistance. Increased expression of this efflux pump has been linked to resistance against various antibiotics, such as ceftazidime, imipenem, ciprofloxacin, gentamicin, tigecycline, and colistin (9, 25, 26).

The expression of the AdeABC efflux pump is regulated by a two-component system mediated by the regulatory genes *adeR* and *adeS* (1, 16). These genes are located upstream of *adeA* and are transcribed in the opposite direction. AdeS functions as a sensor histidine kinase, detecting environmental signals and triggering autophosphorylation. This phosphoryl group is then transferred to the output response (37, 38).

Differences in amino acid sequences were observed between the reference strain (ATCC19606) and the antibiotic resistant strains (H1074 and G560). Numerous studies have reported that alterations in the amino acid sequences of AdeR and AdeS are linked to the overexpression of the AdeABC efflux pump, thus contributing to the increased antibiotic resistance observed in *A. baumannii* (18). Multiple mutations have been observed in the AdeR protein, such as Asp-20⟶Asn on one of the D boxes of the phosphorylation site (54), and Ala-91⟶Val and Pro-116⟶Leu on the signal receiver domain (55). These mutations have been linked to the overexpression of the AdeABC pump in *A. baumannii*. The amino acid sequence positions studied in this research differ from those found in the antibiotic resistant

strains (H1074 and G560). Notable variations include Val-120⟶Ile, Phe-224⟶Leu, and Gln-225⟶Asn, which are located in the receiver domain and DNA binding domain. These mutations may affect the response of the protein after receiving a stimulus, leading to altered functional characteristics in the antibiotic resistant strains. In AdeS, the substitution of Tyr-153⟶Met results in loss of its phosphorylation activity, leading to the constitutive expression of the efflux pump (33). Moreover, the mutation of Ala-94⟶Val in AdeS showed up-regulation of the AdeABC efflux pump, resulting in tigecycline resistance in clinical isolates (56). Other mutations of Gly-103⟶Asp, located between the sensor and Histidine phosphotransfer (DHp) domains (55), and a Gly30⟶Asp substitution in AdeS (57), have also been observed to increase the expression of the AdeABC efflux pump. In contrast to the amino acid sequence positions studied in this research, the antibiotic resistant strains (H1074 and G560) exhibit variations such as Leu-131⟶Phe and Ser-180⟶Ala in the HAMP domain and DHp domain. These specific mutations are known to play a role in the phosphorylation process and have an impact on the regulation of the efflux pump in the antibiotic resistant strains (H1074 and G560). The variation in the amino acid sequence of AdeR and AdeS has implications for the regulation of the efflux pump, which is closely linked to antibiotic resistance in *A. baumannii*. This intriguing observation prompted us to investigate the functions of AdeR, AdeS, and their interactions through a series of experiments, including EMSA, ITC, FRET, and enzymatic activity assays. These experiments were conducted to gain a deeper understanding of the mechanisms underlying the role of AdeR and AdeS in antibiotic resistance.

In a study conducted by Chang et al. in 2016 (1), the binding of AdeR to intercistronic DNA was investigated. They examined both the reference strain of AdeR and an isolate strain obtained from a patient. Interestingly, the AdeR isolated from the patient displayed a distinct amino acid sequence in the DNA binding domain compared to the reference strain. However, both variants of AdeR were found to be

capable of binding to DNA. In our study, we examined three full-length AdeR strains, including the reference strain (ATCC19606) and two antibiotic resistant strains (H1074 and G560), in the context of intercistronic DNA binding. The antibiotic resistant strains (H1074 and G560) exhibited stronger bands compared to the reference strain (ATCC19606). This observation suggests a higher of drug resistance in the antibiotic resistant strains, as AdeR plays a key role in regulating the efflux pump responsible for drug elimination from bacterial cells. The increased band intensity of AdeR in the antibiotic resistant strains indicates stronger binding to DNA, which is linked to AdeR control of the efflux pump. However, the precise binding affinity between AdeR and intercistronic DNA cannot be determined solely based on this observation. To ascertain the binding affinity (K_d) of AdeR to intercistronic DNA, further investigation utilizing the isothermal titration calorimetry (ITC) method is required. In a previous study conducted by Yurong Wen et al. in 2017 (36), they utilized isothermal titration calorimetry (ITC) to examine the binding interactions between AdeR full length (AdeR-FL) and AdeR with a cleaved DNA binding domain (AdeR-DBD). It was found that AdeR-DBD exhibited tighter binding to DNA with a K_d of 20 nM, whereas AdeR-FL had a K_d of 2.2 μM. In our study, we investigated AdeR full length from three strains (ATCC19606, H1074, and G560). Although we aimed to determine the binding affinity with DNA using the ITC method, clear results were not obtained due to limitations in accessing the ITC machine. Further revisions and experiments are required to obtain conclusive findings. However, based on Yurong Wen's study, we can comprehend the role of AdeR in the two-component system, which regulates the efflux pump responsible for drug elimination from bacterial cells. When AdeR binds tightly to DNA, it can influence the control of the efflux pump, potentially leading to increased antibiotic resistance.

As for the investigation of the interaction between AdeR and AdeS using isothermal titration calorimetry (ITC) and fluorescence resonance energy transfer (FRET), there have been no previous reports on this topic. In our study, we

encountered challenges in determining the binding affinity (K_d) between AdeR and AdeS and the strength of their interaction. This limitation was due to difficulties in accessing the necessary tools and equipment. Therefore, future improvements are needed, including revising the experimental protocol for the FRET assay. It is crucial to select the appropriate fluorophores to be attached to our proteins, as this will enable clearer and more accurate measurement of the resulting FRET signal. However, we were able to gather some preliminary information about the interaction between AdeR and AdeS through the enzymatic activity assay, specifically the coupling assay. In this assay, the rate of enzymatic activity was found to be faster in the presence of both AdeR and AdeS compared to AdeS alone (Table 6). The initial rates generated by the antibiotic resistant strains (H1074 and G560) were approximately two times higher than those of the reference strain (ATCC19606), indicating a stronger interaction between AdeR and AdeS in the two-component system (TCS). This interaction is involved in the regulation of the efflux pump, which is associated with bacterial resistance to antibiotics.

In conclusion, this study has revealed that AdeR is capable of binding to intercistronic DNA. Notably, the antibiotic resistant strains exhibited a stronger binding affinity of AdeR to DNA compared to the reference strain, as evident from the intensity of the AdeR-DNA binding bands. However, the exact binding affinity and FRET signaling could not be determined through ITC and FRET experiments. Nevertheless, the coupling assay demonstrated that AdeR and AdeS are capable of interacting, with the antibiotic resistant strains showing approximately twice the interaction strength compared to the reference strain. These findings provide preliminary insights into the functions of AdeR and AdeS, two key proteins in the two-component regulatory system. This system plays a crucial role in increasing resistance to antibiotics by regulating the efflux pump responsible for drug excretion from bacterial cells. However, further investigations are necessary to gain a deeper understanding of the interaction between AdeR and AdeS and its mechanisms. The

results of these studies can serve as a foundation for future research and the development of novel antibiotics to combat *A. baumannii* resistance.

APPENDIX A

MATERIALS AND EQUIPMENT

1.	Autoclave (Scientific promotion co.,LTD.)	Thailand
2.	Balance Precisa XB-220 A (Precisa)	Switzerland
3.	Beaker Duran (Schott)	Germany
4.	Bemis™ Parafilm™ M Laboratory Wrapping Film (Fisher Scientific)	USA
5.	Bottle Assy, PP 500 mL (Beckman coulter)	USA
6.	Centrifuge 4-16KS	Germany
7.	Drying oven Memmert (United instrument co.,LTD.)	Thailand
8.	EMD Millipore 5123 Amicon Stirred Cell Model 8200 (Cole-Parmer Instrument Company)	USA
9.	Fast Performance Liquid Chromatography (FPLC) AKTA pure 25 M1 (Cytiva)	USA
10.	Fluorescence spectrophotometer RF-6000 (Shimadzu)	Japan
11.	Gel documentation EZ Imager (Bio-Rad)	USA
12.	Gel electrophoresis Minigel (Hercuvan lab system)	UK
13.	Isothermal titration calorimetry (ITC) MicroCal PEAQ-ITC (Malvern)	UK
14.	Laminar Scanlaf Mars Safety Class 2	
15.	Magnetic stirrer big-squid (IKA Works do Brasil Ltd.,)	
16.	Microcentrifuge TT-14500 PRO (Hercuvan lab system)	UK
17.	Microcentrifuge tube 1.5 mL (Quality Scientific Plastics)	USA
18.	Minishaker MS1 (IKA Works do Brasil Ltd.,)	
19.	Nanodrop 2000 spectrophotometer (Thermo Scientific)	USA
20.	Pasteur pipettes 3 mL non-sterile (Kartell S.p.a.)	Italy
21.	pH meter Orion star A111(Thermo scientific)	USA
22.	Refrigerated centrifuge AllegraTM 64R (Beckman coulter)	USA
23.	Refrigerator Forma 89000 series (Thermo scientific)	USA

24. SDS PAGE PS300B (Hoefer)	USA
25. Shaker Unimax 1010 (Heidolph)	Germany
26. Sonicator Vibra-cell Ultrasonic Liquid Processer VCX 750 (Biotechnology Research)	Connecticut
27. Spectrophotometer UV-VIS UV-2550 (Shimadzu)	Japan
28. Spin down (Hercuvan lab system)	UK
29. Thermo cycler T100TM (Bio-Rad)	USA
30. Water bath Hetofrig CB60 and Hetomix TBVS (Lab Chiller Heto inter)	
31. Water Purification System Cascada II, I (Pall Life Sciences)	USA

APPENDIX B

BIOLOGICAL/CHEMICAL AGENTS AND REAGENTS

1. 2-mercapto ethanol, C_2H_6SO, (Merck)	Germany
2. Acrylamide/Bis solution 30% (Enzmart biotech)	Thailand
3. Agar powder (HiMedia Laboratories)	India
4. Agarose (Omipur, Calbiochem)	USA
5. Alkaline phosphatase, Quick CIP (BioLabs inc)	England
6. Ammonium Chloride, NH_4Cl (QRëC)	New Zealand
7. Ammoniumperoxodisulfate, $N_2H_8S_2O_8$ (Merck)	Germany
8. Ampicillin (Bio basic canada inc)	Canada
9. Bacteriological peptone (OXOID)	UK
10. Chloramphenicol (Merck)	Germany
11. D-glucose, $C_6H_{12}O_6$ (Univar)	Australia
12. Decon 90 (Decon laboratories Limited)	England
13. Disodium phosphate, Na_2HPO_4 (QRëC)	New Zealand
14. Dithiothreitol, DTT, $C_4H_{10}O_2S_2$ (Cambridge Isotope Laboratories)	USA
15. DNA Ladder (SibEnzyme)	Russia
16. ECOS™ *E.coli* DE3 (Yeastern Biotech Co., LTD.)	China
17. Ethidium bromide, $C_{21}H_{20}BrN_3$, (Tokyo chemical industry)	Japan
18. Ethyl alcohol, C_2H_6O (Emsure)	Germany
19. Ethylene diaminetetra acetic acid, EDTA (QRëC)	New Zealand
20. FavorPrep™ GEL/PCR Purification Mini Kit (Favorgen Biotech Corp)	Taiwan
21. FavorPrep™ Plasmid Extraction Mini Kit (Favorgen Biotech Corp)	Taiwan
22. Formate dehydrogenase (Enzmart biotech)	Thailand
23. Formic acid (98%), CH_2O_2 (Cambridge Isotope Laboratories)	USA
24. G-25 Sephadex (GH Healthcare)	Sweden

25. G-spin™ Total DNA Extraction Kit (iNtRon) Korea
26. Glacial acetic acid (QRëC) New Zealand
27. Glycerol 99.5%, $C_3H_8O_3$ (QRëC) New Zealand
28. Glycine, C_2H_5NO2, (Kemaus chemical) Australia
29. Guanidine hydrochloride, CH_5N_3·HCl, (Omipur Calbiochem) USA
30. Hydrochloric acid, HCl (Riedel-de Haën) USA
31. IMAC-Sepharose (GH Healthcare) Sweden
32. Imidazole 99%, $C_3H_4N_2$ (Alfa Aesar, Thermo Fisher Scientific) USA
33. Isopropyl alcohol, C_3H_8O (Riedel-de Haën) USA
34. Lactose, $C_{12}H_{22}O_{11}$·H_2O, (Kemaus chemical) Australia
35. Magnesium Sulfate, $MgSO_4$ (QRëC) New Zealand
36. Methanol (Cambridge Isotope Laboratories) USA
37. MOPS, Free Acid (Calbiochem) China
38. Nickle (II) Sulfate Hexahydrate, $NiSO_4$·$6H_2O$ (QRëC) New Zealand
39. Nicotinamide adenine dinucleotide, NAD+
    (Fluka biochemika) USA
40. pET22b+ vector
41. Phusion High-Fidelity PCR Kit (Thermo Fisher Scientific) USA
42. Potassium bromide, KBr (QRëC) New Zealand
43. Potassium Dihydrogen Phosphate, KH_2PO_4 (QRëC) New Zealand
44. Potassium hydroxide, KOH (Merck) Germany
45. Prestained Protein marker (Enzmart biotech) Thailand
46. Restriction enzymes *Nde*I, and *Xho*I (BioLabs inc.) England
47. Sephacryl™ S-200 High Resolution
    (GE HealthCare Technologies Inc.) USA
48. Sodium chloride, NaCl (Emsure) Germany
49. Sodium dodecyl sulfate, SDS, $NaC_{12}H_{25}SO_4$,
    (Omipur Calbiochem) USA
50. Sodium hydrosulfite, $Na_2S_2O_4$ (QRëC) New Zealand
51. Sodium hydroxide, NaOH (Merck) Germany
52. Sodium sulfate, Na_2SO_4 (QRëC) New Zealand

53. T4 ligase (ABclonal)	France
54. Tetramethylethylenediamine, TEMED (Merck)	Germany
55. Tris base, Hydroxymethyl aminomethane (Omipur Calbiochem)	USA
56. Yeast extract (OXOID)	UK
57. β-mercaptone (Merck)	Germany

APPENDIX C

SOFTWARE AND DATABASE

1. Bio edit (Manchester Science Parks. UK
2. Chem Draw Ultra 12.0
   (PerkinElmer, Macintosh, and Microsoft Windows USA
3. KaleidaGraph (Synergy International Syxtem, Inc.) USA

APPENDIX D

REAGENT PREPARATION

1. 10X SDS

Tris base (hydroxymethyl) aminomethane	30.3 g
Glycine	144.4 g
SDS	10 g
De-ionized water (to be 1 L)	

2. 5X TBE

Tris base (hydroxymethyl) aminomethane	54 g
Boric acid (crystal)	27.5 g
EDTA	3.72 g
De-ionized water (to be 1 L)	

3. LB broth media (1 L)

Bacteriological peptone	10 g
Yeast extract	5 g
NaCl	10 g
Distilled water (to be 1 L)	

4. LB Agar (2%)

LB broth	100 ml
Bacteriological agar	2 g

5. Reagents for auto-induction media

   a. ZY medium (1 L)

Bacteriological peptone	10 g
Yeast extract	5 g
Distilled water (to be 1 L)	

b. 50X MPS (1 L)

1.25 M Na_2HPO_4	177 g
1.25 M KH_2PO_4	170 g
2.5 M NH_4Cl	133 g
Distilled water (to be 1 L)	

c. 50X 5052 (1 L)

25 % Glycerol	250 g
2.5 % Glucose	25 g
1 % Lactose	100 g
Distilled water (to be 1 L)	

d. 1 M $MgSO_4$ (100 ml)

$MgSO_4 \cdot 7H_2O$	24.65 g
Distilled water (to be 100 ml)	

e. 1 M Na_2SO_4 (100 ml)

Na_2SO_4	14.2 g
Distilled water (to be 100 ml)	

f. 40% glucose (w/v) (100 ml)

Glucose	40 g
Distilled water (to be 100 ml)	

6. 70% Ethanol

100% Ethanol	70 ml
Sterile water	30 ml

REFERENCES

1. Chang T-Y, Huang B-J, Sun J-R, Perng C-L, Chan M-C, Yu C-P, et al. AdeR protein regulates *adeABC* expression by binding to a direct-repeat motif in the intercistronic spacer. Microbiological Research. 2016;183:60-7.

2. Howard A, O'Donoghue M, Feeney A, Sleator RD. *Acinetobacter baumannii*. Virulence. 2012;3(3):243-50.

3. Cerqueira GM, Peleg AY. Insights into *Acinetobacter baumannii* pathogenicity. IUBMB Life. 2011;63(12):1055-60.

4. Wongsuk T, Boonsilp S, Homkaew A, Thananon K, Oonanant W. Whole genome sequence of pan drug-resistant clinical isolate of *Acinetobacter baumannii* ST1890. PLOS ONE. 2022;17(3):e0264374.

5. Organization WH. 2020 Antibacterial agents in clinical and preclinical development: an overview and analysis. Geneva 2021 [Available from: https://www.who.int/publications/i/item/9789240047655.

6. Alsan M, Klompas M. *Acinetobacter baumannii*: An Emerging and Important Pathogen. J Clin Outcomes Manag. 2010;17(8):363-9.

7. Ibrahim S, Al-Saryi N, Al-Kadmy IMS, Aziz SN. Multidrug-resistant *Acinetobacter baumannii* as an emerging concern in hospitals. Molecular Biology Reports. 2021;48(10):6987-98.

8. Gheorghe I, Barbu IC, Surleac M, Sârbu I, Popa LI, Paraschiv S, et al. Subtypes, resistance and virulence platforms in extended-drug resistant *Acinetobacter baumannii* Romanian isolates. Scientific Reports. 2021;11(1):13288.

9. Lee CR, Lee JH, Park M, Park KS, Bae IK, Kim YB, et al. Biology of *Acinetobacter baumannii*: Pathogenesis, Antibiotic Resistance Mechanisms, and Prospective Treatment Options. Front Cell Infect Microbiol. 2017;7:55.

10. Pandey N CM. Beta Lactam Antibiotics. 2022 [updated 2022 Feb 5; cited 2022. Available from: https://www.ncbi.nlm.nih.gov/books/NBK545311/.

11. Girija As S, Priyadharsini JV. CLSI based antibiogram profile and the detection of MDR and XDR strains of *Acinetobacter baumannii* isolated from urine samples. Med J Islam Repub Iran. 2019;33:3.

12. Vila J, Martí S, Sánchez-Céspedes J. Porins, efflux pumps and multidrug resistance in *Acinetobacter baumannii*. Journal of Antimicrobial Chemotherapy. 2007;59(6):1210-5.

13. Yılmaz Ç, Özcengiz G. Antibiotics: Pharmacokinetics, toxicity, resistance and multidrug efflux pumps. Biochemical Pharmacology. 2017;133:43-62.

14. Li XZ, Nikaido H. Efflux-mediated drug resistance in bacteria: an update. Drugs. 2009;69(12):1555-623.

15. Magnet S, Courvalin P, Lambert T. Resistance-Nodulation-Cell Division-Type Efflux Pump Involved in Aminoglycoside Resistance in *Acinetobacter baumannii* Strain BM4454. Antimicrobial Agents and Chemotherapy. 2001;45(12):3375-80.

16. Wieczorek P, Sacha P, Hauschild T, Zórawski M, Krawczyk M, Tryniszewska E. Multidrug resistant *Acinetobacter baumannii*--the role of AdeABC (RND family) efflux pump in resistance to antibiotics. Folia Histochemica et Cytobiologica. 2008;46(3):257-67.

17. Blair JMA, Piddock LJV. Structure, function and inhibition of RND efflux pumps in Gram-negative bacteria: an update. Current Opinion in Microbiology. 2009;12(5):512-9.

18. Yoon E-J, Courvalin P, Grillot-Courvalin C. RND-Type Efflux Pumps in Multidrug-Resistant Clinical Isolates of *Acinetobacter baumannii*: Major Role for AdeABC Overexpression and AdeRS Mutations. Antimicrobial Agents and Chemotherapy. 2013;57(7):2989-95.

19. Coyne S, Rosenfeld N, Lambert T, Courvalin P, Périchon B. Overexpression of Resistance-Nodulation-Cell Division Pump AdeFGH Confers Multidrug Resistance in *Acinetobacter baumannii*. Antimicrobial Agents and Chemotherapy. 2010;54(10):4389-93.

20. Coyne S, Courvalin P, Périchon B. Efflux-Mediated Antibiotic Resistance in *Acinetobacter* spp. Antimicrobial Agents and Chemotherapy. 2011;55(3):947-53.

21. Hou PF, Chen XY, Yan GF, Wang YP, Ying CM. Study of the Correlation of Imipenem Resistance with Efflux Pumps AdeABC, AdeIJK, AdeDE and AbeM in Clinical

Isolates of *Acinetobacter baumannii*. Chemotherapy. 2012;58(2):152-8.

22. Xu CF, Bilya SR, Xu W. adeABC efflux gene in *Acinetobacter baumannii*. New Microbes and New Infections. 2019;30:100549.

23. Tierney AR, Rather PN. Roles of two-component regulatory systems in antibiotic resistance. Future Microbiology. 2019;14(6):533-52.

24. De Silva PM, Kumar A. Signal Transduction Proteins in *Acinetobacter baumannii*: Role in Antibiotic Resistance, Virulence, and Potential as Drug Targets. Front Microbiol. 2019;10:49.

25. Ayoub Moubareck C, Hammoudi Halat D. Insights into *Acinetobacter baumannii*: A Review of Microbiological, Virulence, and Resistance Traits in a Threatening Nosocomial Pathogen. Antibiotics. 2020;9(3):119.

26. Fishbain J, Peleg AY. Treatment of *Acinetobacter* Infections. Clinical Infectious Diseases. 2010;51(1):79-84.

27. Peleg AY, Adams J, Paterson DL. Tigecycline Efflux as a Mechanism for Nonsusceptibility in *Acinetobacter baumannii*. Antimicrobial Agents and Chemotherapy. 2007;51(6):2065-9.

28. Havenga B, Reyneke B, Waso-Reyneke M, Ndlovu T, Khan S, Khan W. Biological Control of *Acinetobacter baumannii*: In Vitro and In Vivo Activity, Limitations, and Combination Therapies. Microorganisms. 2022;10(5):1052.

29. Sun J, Deng Z, Yan A. Bacterial multidrug efflux pumps: Mechanisms, physiology and pharmacological exploitations. Biochemical and Biophysical Research Communications. 2014;453(2):254-67.

30. Abbott I, Cerqueira GM, Bhuiyan S, Peleg AY. Carbapenem resistance in *Acinetobacter baumannii*: laboratory challenges, mechanistic insights and therapeutic strategies. Expert Review of Anti-infective Therapy. 2013;11(4):395-409.

31. Blair JMA, Webber MA, Baylay AJ, Ogbolu DO, Piddock LJV. Molecular mechanisms of antibiotic resistance. Nature Reviews Microbiology. 2015;13(1):42-51.

32. Piddock LJV. Clinically Relevant Chromosomally Encoded Multidrug Resistance Efflux Pumps in Bacteria. Clinical Microbiology Reviews. 2006;19(2):382-402.

33. Marchand I, Damier-Piolle L, Courvalin P, Lambert T. Expression of the RND-Type Efflux Pump AdeABC in *Acinetobacter baumannii* Is Regulated by the AdeRS Two-

Component System. Antimicrobial Agents and Chemotherapy. 2004;48(9):3298-304.

34. Haubrich BA, Swinney DC. Enzyme Activity Assays for Protein Kinases: Strategies to Identify Active Substrates. Curr Drug Discov Technol. 2016;13(1):2-15.

35. West AH, Stock AM. Histidine kinases and response regulator proteins in two-component signaling systems. Trends Biochem Sci. 2001;26(6):369-76.

36. Wen Y, Ouyang Z, Yu Y, Zhou X, Pei Y, Devreese B, et al. Mechanistic insight into how multidrug resistant *Acinetobacter baumannii* response regulator AdeR recognizes an intercistronic region. Nucleic Acids Research. 2017;45(16):9773-87.

37. Ouyang Z, Zheng F, Zhu L, Felix J, Wu D, Wu K, et al. Proteolysis and multimerization regulate signaling along the two-component regulatory system AdeRS. iScience. 2021;24(5).

38. Bhate Manasi P, Molnar Kathleen S, Goulian M, DeGrado William F. Signal Transduction in Histidine Kinases: Insights from New Structures. Structure. 2015;23(6):981-94.

39. Uversky VN. Use of fast protein size-exclusion liquid chromatography to study the unfolding of proteins which denature through the molten globule. Biochemistry. 1993;32(48):13288-98.

40. Madadlou A, O'Sullivan S, Sheehan D. Fast protein liquid chromatography. Protein Chromatography: Methods and Protocols. 2011:439-47.

41. Hellman LM, Fried MG. Electrophoretic mobility shift assay (EMSA) for detecting protein–nucleic acid interactions. Nature Protocols. 2007;2(8):1849-61.

42. Holden NS, Tacon CE. Principles and problems of the electrophoretic mobility shift assay. Journal of Pharmacological and Toxicological Methods. 2011;63(1):7-14.

43. Wang Y, Wang G, Moitessier N, Mittermaier AK. Enzyme Kinetics by Isothermal Titration Calorimetry: Allostery, Inhibition, and Dynamics. Front Mol Biosci. 2020;7:583826.

44. Lin K, Wu G. Isothermal Titration Calorimetry Assays to Measure Binding Affinities In Vitro. In: Hergovich A, editor. The Hippo Pathway: Methods and Protocols. New York, NY: Springer New York; 2019. p. 257-72.

45. Lee WC, Park J, Balasubramanian PK, Kim Y. Elucidation of the crystal structure of FabD from the multidrug-resistant bacterium *Acinetobacter baumannii*. Biochemical

and Biophysical Research Communications. 2018;505(1):208-14.

46. Draughn GL, Milton ME, Feldmann EA, Bobay BG, Roth BM, Olson AL, et al. The Structure of the Biofilm-controlling Response Regulator BfmR from *Acinetobacter baumannii* Reveals Details of Its DNA-binding Mechanism. Journal of Molecular Biology. 2018;430(6):806-21.

47. Verma V, Testero SA, Amini K, Wei W, Liu J, Balachandran N, et al. Hydrolytic Mechanism of OXA-58 Enzyme, a Carbapenem-hydrolyzing Class D β-Lactamase from *Acinetobacter baumannii*. Journal of Biological Chemistry. 2011;286(43):37292-303.

48. McFarlane CR, Murray JW. A Sensitive Coupled Enzyme Assay for Measuring Kinase and ATPase Kinetics Using ADP-Specific Hexokinase. Bio Protoc. 2020;10(9):e3599.

49. Carter SG, Karl DW. Inorganic phosphate assay with malachite green: An improvement and evaluation. Journal of Biochemical and Biophysical Methods. 1982;7(1):7-13.

50. Sherwood AR, Paasch BC, Worby CA, Gentry MS. A malachite green-based assay to assess glucan phosphatase activity. Anal Biochem. 2013;435(1):54-6.

51. A Geno Technology IG-B. Malachite Green Phosphate Assay.

52. Kraithong T, Sucharitakul J, Buranachai C, Jeruzalmi D, Chaiyen P, Pakotiprapha D. Real-time investigation of the roles of ATP hydrolysis by UvrA and UvrB during DNA damage recognition in nucleotide excision repair. DNA Repair (Amst). 2021;97:103024.

53. Wu L, Huang C, Emery BP, Sedgwick AC, Bull SD, He X-P, et al. Förster resonance energy transfer (FRET)-based small-molecule sensors and imaging agents. Chemical Society Reviews. 2020;49(15):5110-39.

54. Higgins PG, Schneiders T, Hamprecht A, Seifert H. In vivo selection of a missense mutation in adeR and conversion of the novel bla OXA-164 gene into bla OXA-58 in carbapenem-resistant *Acinetobacter baumannii* isolates from a hospitalized patient. Antimicrobial agents and chemotherapy. 2010;54(12):5021-7.

55. Hornsey M, Loman N, Wareham DW, Ellington MJ, Pallen MJ, Turton JF, et al. Whole-genome comparison of two *Acinetobacter baumannii* isolates from a single patient, where resistance developed during tigecycline therapy. Journal of antimicrobial chemotherapy. 2011;66(7):1499-503.

56. Hornsey M, Ellington MJ, Doumith M, Thomas CP, Gordon NC, Wareham DW, et al. AdeABC-mediated efflux and tigecycline MICs for epidemic clones of *Acinetobacter baumannii*. J Antimicrob Chemother. 2010;65(8):1589-93.

57. Coyne S, Guigon G, Courvalin P, Périchon B. Screening and quantification of the expression of antibiotic resistance genes in *Acinetobacter baumannii* with a microarray. Antimicrobial agents and chemotherapy. 2010;54(1):333-40.

VITA

NAME	KONRAWEE THANANON
DATE OF BIRTH	15 September 1994
PLACE OF BIRTH	Thailand
INSTITUTIONS ATTENDED	2017: B. Sc. (Biotechnology), King Mongkut's University of Technology North Bangkok Present: M. Sc. (Graduate School, Medical Microbiology), Chulalongkorn University
HOME ADDRESS	34/35, Moobaan Nonsi 4, Mueang Nonthaburi, Nonthaburi 11000
PUBLICATION	Wongsuk, T., Boonsilp, S., Homkaew, A., Thananon, K., & Oonanant, W. (2022). Whole genome sequence of pan drug-resistant clinical isolate of Acinetobacter baumannii ST1890. PloS one, 17(3), e0264374. https://doi.org/10.1371/journal.pone.0264374 Thananon, K., Sucharitakul, J., Oonanant, W., & Ritprajak, P. (2022) Study of protein interaction between AdeR (response regulator) and AdeS (histidine kinase) in two-component antibiotic sensor of Acinetobacter baumannii. In the 17th International Symposium of the Protein Society of Thailand